Table 1. Primers used for the amplification of *ADAMTS13* exons and intron–exon boundaries

Exon (size, bp)	Forward primer	Reverse primer	Product, bp
1 (549)	GATTGCCAGGCCGTTTGTGAT	GCAAACCCCAAAGCTGATGTA	768
2 (67)	CCTCGGTCTCCCCAAGTGTTA	GAACCCTGGCCTGGCTGGAAC	348
3 (158)	GGTGGGGGTGACACGCAATGT	CCAGGGGAGGGAGGGAGAAGA	437
4 (84)	TGTTTTCCTTGCGTTAGTTGG	GAGGATGGAGATGCGATGACT	382
5–6 (125, 147)	AACAAACCGACCGCAGTCAGC	GGTTCCCCTGTCCTCACACCT	638
7 (138)	GCTGGCGCTGCGGCACTAGGG	GTTGGACGGAGGGGTGGGTTG	399
8 (163)	ACTCCTCCGTCCCGCCTCCTC	GGCCCAGTCAAACAAAAATGT	446
9 (105)	GTGCAGAGTGTTGGCTGTGTC	CTCTGCCCCATACTGGTCCTG	334
10–11 (152, 64)	TGAGGATGTTGGGGGACTCTC	CAAATGTGTCCTGGTGTGAAC	512
12 (127)	TGAGGCCACACCCACATCTTG	ATGCCAGAGCCTGAACCACTT	366
13 (149)	ATAGAAACCCTTGCCCCAGAT	ATCCTTTTCCCCAGCACCACT	390
14 (121)	CAGGGCTGCAGAGTCATTGAG	GAAGGGTGGCGAAGTGGAAGA	358
15 (81)	CTCCCTTTGTCTGTGGTGTGG	ACTATCAAGCCTGAGGGTGGT	279
16 (182)	GGGACCCCGGGAAGGAGAGTC	GTAAGTGACCGCTGAATGAAT	393
17–18 (136, 130)	GGCCAGGCTGGAGTGCTATGT	CAGAATGGGGGCACTCACAGA	770
19 (186)	ACCAGCCTGTGATTCGGTTGT	AGGAACTCTGACAGCAGCACT	548
20 (190)	CTCTTTGGGCTCCTGGATGTT	CAATGGGTGCTCCTCGTTCTC	386
21 (121)	AAGGATACCCGCTGCGAGACC	AGCCAATCAACACCCACATTT	489
22 (130)	CCATGCGGGCCTTATGTGCTA	TCTGGGTTGCAGTCCTCAAAG	439
23 (183)	GGGGGCCTCCAGAAAGAGAAC	GTGTTGCCCAGGTTGGACTTG	476
24 (205)	GGCTCAGTGGCTGCACTTTCC	TCCAGCGTCCCCAAACCTAAG	576
25 (319)	GACAGGGACCCAGACTTGAAT	AAGTTACTTCCCCTTGATAGT	729
26 (147)	CTGCATGTGCCCCCTCTTGCT	TGGGCACATCACTTAATCTCT	574
27 (177)	GTGCATTCCCACCTGTAGTTT	TCCCTGGCACGTGCAGACTGA	583
28 (185)	CCAGAGCCCAGAACATTTAGC	GCCACTATTTCACTCTTGTAG	581
29 (412)	GTGTCCTTGGGGAAGTGATGT	GATTGGATTTTCTTCCTGGAT	757

and A1033T) in 92 unrelated normal control DNA samples, although their effects on VWF-CP activity have not been assessed (22).

Here, we report three missense and one nonsense novel mutations in Japanese families with congenital TTP. Altered activities of the expressed recombinant VWF-CP mutants accounted for the patients' symptoms. Notably, one of the missense mutations is a common SNP with approximately 10% heterozygosity.

Materials and Methods

Sequencing of *ADAMTS13* Gene. All experiments using human materials were performed with the permission of the ethics committees at the National Cardiovascular Center, Yodogawa Christian Hospital, and Sapporo Kosei General Hospital. Human genomic DNA was isolated from whole blood by using an automated nucleic acid isolation system, NA-3000 (Kurabo, Japan). All exons of the *ADAMTS13* gene, including the intron–exon boundaries, were PCR-amplified with corresponding intron primers (Table 1) by using either FastStart *Taq*DNA polymerase (Roche Diagnostics), the GC-RICH PCR system (Roche Diagnostics), or HotStarTaq DNA polymerase (Qiagen, Chatsworth, CA). Products were sequenced in both directions by using a BigDye Terminator Kit (Applied Biosystems) and a 3700 DNA Analyzer (Applied Biosystems).

Transient Expression of VWF-CP. To produce recombinant VWF-CP, the ORF of human *ADAMTS13* was PCR-amplified from cDNA (18) with or without a C-terminal FLAG (DYKDDDDK) tag sequence. This fragment was inserted into a mammalian expression vector, pCAGG (28). We used PCR-based single-nucleotide mutagenesis to create the R268P, Q448E, Q449stop, P475S, and C508Y mutants. The direction and sequence of all inserts were confirmed by sequencing.

HeLa cells were cultured in DMEM (Invitrogen) supplemented with 10% FBS (Invitrogen) on 60-mm dishes in humidified air with 5% CO_2 at 37°C. Two micrograms of each expression plasmid was transfected into subconfluent cells by using FuGENE6 (Roche Diagnostics). After a 4-h incubation, culture media were replaced with 2.5 ml of serum-free OPTI-MEM I (Invitrogen) and incubated for 44 h. The media were then collected and centrifuged to remove any cellular residue. The cells were washed with PBS and lysed with 300 μl of SDS-sample buffer (10 mM Tris·HCl/2% SDS/50 mM DTT/mM EDTA/0.02% bromophenol blue/6% glycerol, pH 6.8).

Western Blot Analysis. The collected culture media and cell lysates were subjected to SDS/PAGE (2–15% gradient) and transferred to a poly(vinylidene difluoride) membrane (Bio-Rad). After blocking with 3% skim milk, the membrane was incubated with 1 μg/ml anti-FLAG M2 mAb (Sigma) and then with 0.1 μg/ml peroxidase-labeled goat anti-mouse IgG (Kirkegaard & Perry Laboratories). Chemiluminescence was developed by using the Western Lightning Chemiluminescence Reagent Plus (Perkin–Elmer), and detected on an image analyzer LAS-1000 PLUS (Fujifilm).

Deglycosylation. The culture media and cell lysates were treated with peptide:N-glycosidase F (PNGase F, NEB, Beverly, MA). Ten microliters of the samples was boiled for 10 min in 1× denaturing buffer, followed by a 1-h incubation with or without 1,000 units of PNGase F in 1× G7 buffer and 1% Nonidet P-40. These samples were then subjected to Western blot analysis.

Purification of VWF. Human VWF was purified by two-column chromatographic steps. Fresh frozen plasma was thawed overnight at 4°C to obtain cryoprecipitate by centrifugation. The cryoprecipitate was dissolved in 25 mM Tris buffer (pH 7.3) containing 0.5 mM EDTA, 0.15 M NaCl, and 1 mM PMSF, and applied to a Gelatin Sepharose 4B (Amersham Pharmacia) column to remove fibronectin. The flowthrough fraction was

precipitated by 40% saturated ammonium sulfate, and the precipitate was dissolved in a buffer (20 mM imidazole/20 mM ε-aminocaproic acid/1 M NaCl/10 mM sodium citrate, pH 6.5). The sample was applied to a Sepharose 4B (Amersham Pharmacia) gel filtration column to remove factor VIII and a small amount of VWF-CP. VWF was eluted in the void volume.

Analysis of VWF-Multimeric State. The culture media of HeLa cells expressing recombinant VWF-CP were concentrated to one-tenth the original volume by using Centricon YM-30 (Millipore). VWF-CP activity was assayed as described by Furlan *et al.* (29) with slight modification (5). In brief, 8 μl of concentrated culture medium was added to 92 μl of purified VWF (1 μg) dissolved in reaction buffer (1.5 M urea/5 mM Tris·HCl/10 mM $BaCl_2$/1 mM PMSF/0.05% NaN_3, pH 8.0), and incubated at 37°C for 24 h. Next, 10 μl of 100 mM EDTA (pH 8.0) quenched the reaction. Under these conditions, the Y842-M843 peptidyl bond of VWF is cleaved specifically (14). A portion of each reaction mixture was analyzed by SDS-agarose gel electrophoresis; the multimeric state of VWF was visualized by chemiluminescent Western blot analysis by using anti-VWF primary antibodies.

Results

Mutations in *ADAMTS13* Gene of Two Japanese Families. To amplify the 29 exons of the *ADAMTS13* gene, we designed and synthesized 26 pairs of oligonucleotide primers on the basis of the two public genomic (GenBank accession nos. AL158826 and AC002325) and cDNA sequences (GenBank accession nos. AB069698, AF414401, and AY055376) (Table 1). PCR using these primers successfully amplified all exons, despite the failure of the previous report to obtain exon 7 (22). The PCR products (279–770 bp in size) amplified from the genomic DNA of seven individuals in two unrelated USS families (Fig. 1) were fully sequenced. Single-nucleotide mutations at 10 sites were identified (Table 2).

Five silent mutations, 420T>C, 546C>T, 1716G>A, 2280C>T, and 4221C>A, were discovered in the two families examined. The nucleotides are numbered from the A of the initiation Met codon. These silent mutations will not be associated with the structure and function of VWF-CP itself, although it may affect the expression level through gene transcription or RNA processing. Four of them, excluding 546C>T, have been reported as SNPs (22). We also identified five additional mutations: four missense mutations in family A and one nonsense mutation in family B. Among these, the 1342C>G mutation (Q448E) has been reported as an SNP (22). The effect of this mutation on VWF-CP activity, however, has not been described. Then, we assessed the effects of the 1342C>G (Q448E) mutation and four additional mutations, 803G>C (R268P), 1345C>T (Q449stop), 1423C>T (P475S), and 1523G>A (C508Y), on VWF-CP activity, comparing the plasma VWF-CP activities of seven individuals in the two USS families with their genotypes.

Assessment of the Mutations in Family A. The plasma VWF-CP activities of family A were reported (5) (Fig. 1*A*). The proband with USS possessed an activity below 3% of normal, a detection limit of the assay. The VWF-CP activities in proband's mother and sister were moderately decreased to 36% and 30% of normal levels, respectively. Because the activity in normal subjects ranged from approximately 60% to 150% of pooled normal plasma (30), we currently consider the individuals with 30–70% activity to be heterozygotes if they have no inhibitors. Subclinical father had extremely low activity (5.6%).

We discovered four missense mutations in this family: R268P, Q448E, P475S, and C508Y. All of these mutations were detected as heterozygous; no other mutations in the gene were identified. Haplotype was determined by linkage analysis. The proband possessed the PQPC/REPY (underlines show the mutated positions) diplotype configuration, implying that the R268P mutation completely abrogated VWF-CP activity as well as either Q448E or C508Y (or their combination). Because Q448E and C508Y were located on a single allele, the effect of each of these two mutations was indistinguishable. The diplotype of proband's mother, RQPC/REPY, was consistent with the intermediate effect of the Q448E/C508Y mutation. The diplotype of his sister, RQPC/RQSC, suggested that the P475S mutation also results in decreased VWF-CP activity.

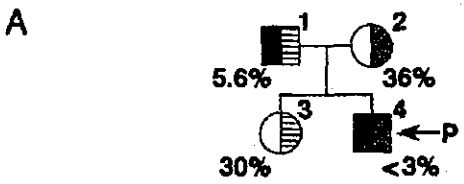

	R268	Q448	P475	C508	Haplotype
1	R/P	Q/Q	P/S	C/C	PQPC/RQSC
2	R/R	Q/E	P/P	C/Y	RQPC/REPY
3	R/R	Q/Q	P/S	C/C	RQPC/RQSC
4	R/P	Q/E	P/P	C/Y	PQPC/REPY

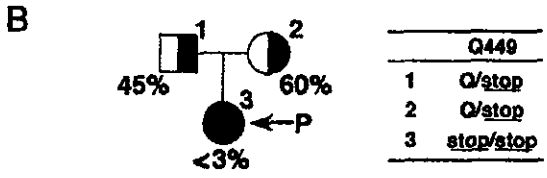

	Q449
1	Q/stop
2	Q/stop
3	stop/stop

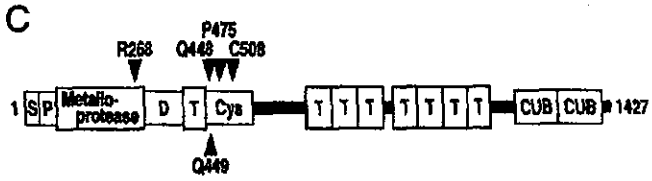

Fig. 1. Pedigrees and haplotypes of patient families. (*A*) Family A. (*B*) Family B. Squares and circles indicate male and female, respectively, and arrows indicate the probands. The VWF-CP activities determined by multimer analysis, as reported (5), are shown as a percentage of the normal control. Missense and nonsense mutations found in the *ADAMTS13* gene are shown in one-letter amino acid residues numbering from the initiation methionine. (*C*) Schematic domain structure of VWF-CP. S, signal peptide; P, propeptide; D, disintegrin-like; T, TSP1; Cys, Cys-rich.

Assessment of the Mutation in Family B. The plasma VWF-CP activities of family B were also reported (5) (Fig. 1*B*). The proband with USS possessed VWF-CP activity less than 3% of normal. The activities of proband's father and mother were moderately decreased to 45% and 60% of control levels, respectively. They did not contain inhibitors of VWF-CP activity.

In this family, we identified only one nonsense mutation, Q449stop. The proband was homozygous for the mutation, whereas each of the parents was heterozygous. Therefore, the Q449stop seriously affects VWF-CP activity.

Expression of Recombinant VWF-CP and Its Mutants. To confirm the functional effects of the identified mutations, wild-type (WT) and mutant human VWF-CP forms were transiently expressed in HeLa cells. The FLAG-tag sequence was added to the C terminus to aid in immunochemical detection. Transient expression of WT VWF-CP produced a single immunoreactive band with a molecular mass of approximately 230 kDa in culture medium (Fig. 2 *Upper*). Because the band was not detected in

Table 2. *ADAMTS13* mutations in two TTP families

Exon	Family	Nucleotide	Amino acid	Frequency	Heterozygosity
5	A	420 T>C*	Silent	ND	–
6	A	546 C>T	Silent	ND	–
7	A	803 G>C	R268P	GG:364, CG:0, CC:0	<0.3%
12	A	1342 C>G*	Q448E	CC:321, CG:125, GG:8	31.2%
12	B	1345 C>T	Q449stop	CC:364, CT:0, TT:0	<0.3%
12	A	1423 C>T	P475S	CC:328, CT:35, TT:1	9.6%
13	A	1523 G>A	C508Y	GG:364, AG:0, AA:0	<0.3%
15	A	1716 G>A*	Silent	ND	–
19	A	2280 C>T*	Silent	ND	–
29	A, B	4221 C>A*	Silent	ND	–

ND, not determined.
*Reported by Levy *et al.* (22).

untransfected cells, this protein is considered to be the expected product of the transfected plasmid. Upon expression of the Q448E and P475S mutants, a single band of the same size appeared in culture medium. The Q449stop mutant exhibited a 54-kDa band. This finding suggested that each of these mutants was secreted from cells. No bands, however, were detected in the culture medium of cells expressing either the R268P or C508Y mutants. As these mutants were synthesized within the cells (Fig. 2 *Lower*), both the R268P and C508Y mutations affected some aspect of the secretion pathway possibly including changes in protein folding and stability. This observation explains the absence of activity in the plasma of family A members with these alleles.

Side-by-side analysis of WT bands in both culture media and cell lysates clearly demonstrated significant differences in size; the protein possessed a molecular mass of 230 kDa in media vs. 200 kDa in lysates (Fig. 3). To examine the possibility that this difference was caused by differences in glycosylation structure, both were treated with PNGase F that removes N-linked carbohydrate residues from polypeptides. This treatment lowered the apparent molecular masses of the bands in the medium and lysate to 180 and 170 kDa, respectively, indicating both were N-glycosylated. Even after PNGase treatment, however, a 10-kDa difference between them remained. This difference may result from a posttranslational modification such as O-linked glycosylation.

Because Q448E, Q449stop, and P475S mutants were efficiently secreted (Fig. 2), the deleterious effect of these mutations on plasma VWF-CP activity cannot be explained by abnormal secretion. Therefore, we examined the VWF-CP activity of these recombinant proteins.

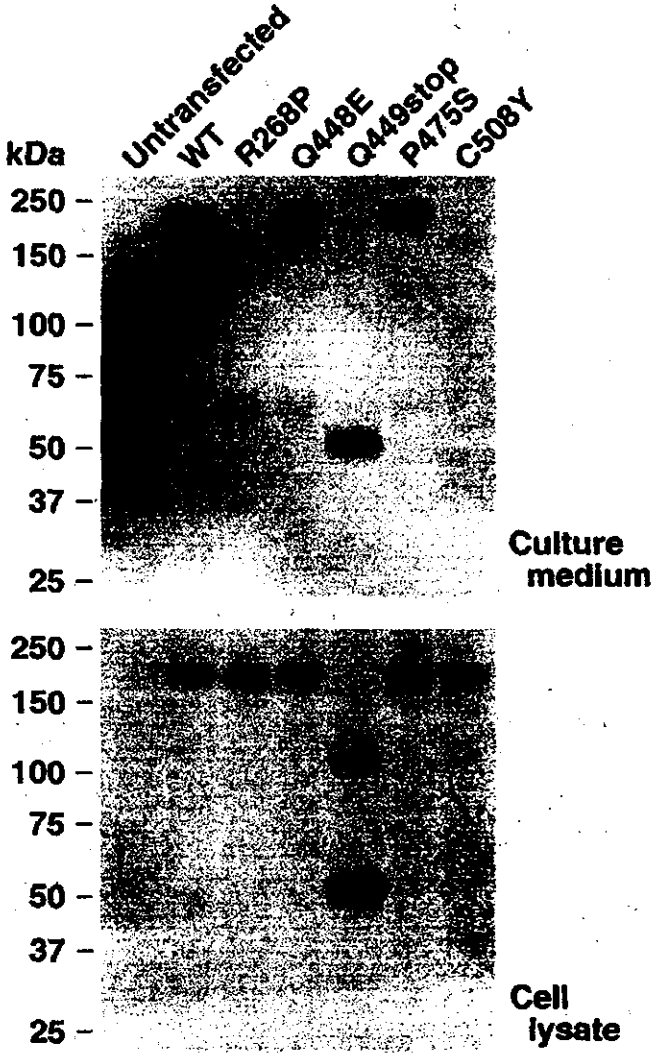

Fig. 2. Expression of recombinant VWF-CP. The human WT VWF-CP and mutants with C-terminal FLAG-tag were transiently expressed in HeLa cells. The culture media (*Upper*) and cell lysates (*Lower*) were analyzed by Western blot with an anti-FLAG antibody. The representative of three repetitive experiments is shown. The sizes of the protein standards are indicated at the left.

Cleavage of VWF by Recombinant VWF-CPs. The enzymatic activity of the recombinant VWF-CPs was measured by degradation of VWF multimers. Purified VWF was incubated with the conditioned culture medium, and the multimeric state of VWF was determined by Western blot analysis after SDS-agarose electro-

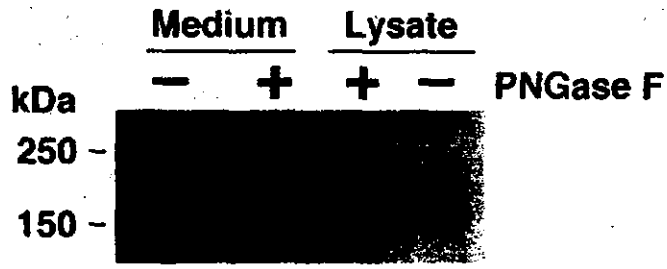

Fig. 3. N-glycosidase treatment of recombinant VWF-CP. FLAG-tagged WT VWF-CP derived from culture media and cell lysates were treated with PNGase F and analyzed by Western blot with an anti-FLAG antibody. The sizes of the protein standards are indicated at the left.

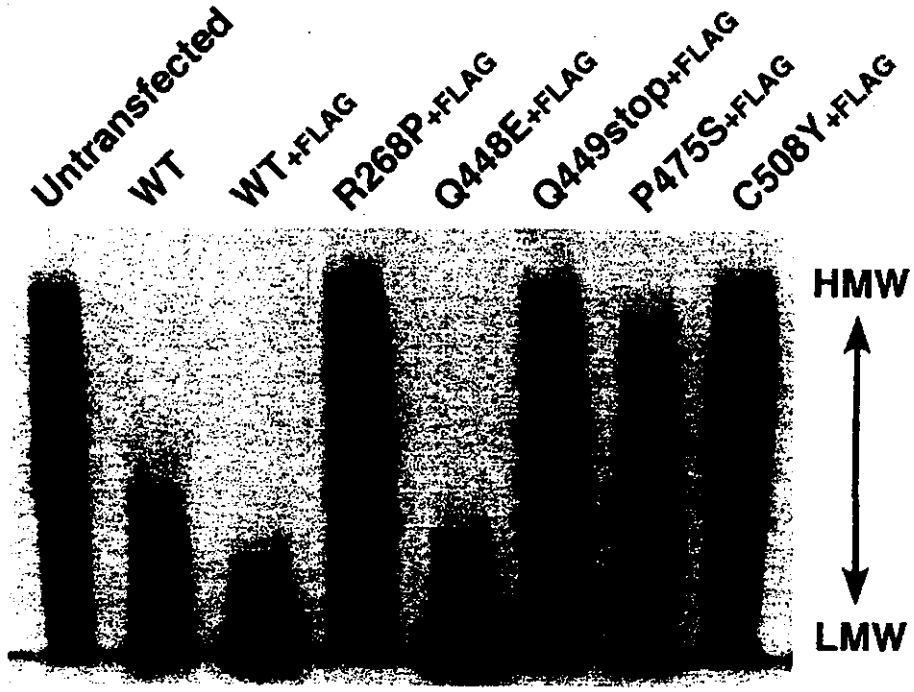

Fig. 4. Cleavage of VWF multimers. The culture media of HeLa cells either untransfected or transfected with VWF-CP expression plasmids were incubated with purified VWF. A portion of each reaction mixture was then separated by SDS-agarose gel electrophoresis. The multimeric states of VWF were visualized by Western blot analysis with an anti-VWF antibody. The representative of three repetitive experiments is shown. HMW, high molecular weight; LMW, low molecular weight.

phoresis (Fig. 4). After the incubation of VWF with the medium of untransfected cells, protein ladders extended into the high molecular weight area, indicating no VWF-cleaving activity in the medium (Fig. 4, Untransfected). In contrast, the ladders diminished after incubation with WT conditioned medium, demonstrating the VWF-CP activity of the recombinant protein. Because the FLAG-tagged version (WT+FLAG) also possessed cleaving activity, a possible interference effect of the tag was excluded. For R268P and C508Y, no degradation was observed, consistent with the absence of secretion into the medium (Fig. 2).

The Q448E mutant was fully active in comparison with the WT and WT+FLAG. This mutation was reported as an SNP in the *ADAMTS13* gene, although its influence on VWF-CP activity has not been described (22). Our data suggest that the Q448E polymorphism is not involved in alterations of biological activity.

A slight loss of high molecular weight multimers was observed in P475S, suggesting that this mutant had low but significant activity. In the Q449stop, the loss of multimers in high molecular weight was not observed, but the intensities of ladders in the low molecular weight area were increased like the other active mutants such as Q448E and P475S. Neither inactive R268P nor C508Y produced these lower ladders. This finding suggests that the Q449stop mutant possessed quite low VWF-CP activity. Thus, the five mutations we identified can be classified into three categories: (*i*) Q448E, with no difference from the WT VWF-CP; (*ii*) R268P and C508Y, with no activity because of secretion problems; and (*iii*) Q449stop and P475S, with very low activity despite normal secretion.

Frequency of the Mutations in Japanese. To investigate the frequencies of the five mutations, we sequenced exons 7, 12, and 13 of *ADAMTS13* from genomic DNAs isolated from 364 Japanese individuals without TTP (Table 2). The R268P, Q449stop, and C508Y mutations did not appear in the large panel, indicating these critical mutations were rare (<0.3% heterozygosity). We found, however, that the other two mutations, Q448E and P475S, were common. The SNP of Q448E has already been reported, although its frequency is not known (22). Of 364 individuals, we identified 125 heterozygotes and eight homozygotes. The allele frequency and heterozygosity were then calculated to be 19.4% and 31.2%, respectively. The Q448E polymorphism, however, is not associated with reduced VWF-CP activity.

The P475S mutation was also common. Of 364 individuals, 35 were heterozygotes and one was a homozygote. Therefore, the allele frequency and heterozygosity were 5.1% and 9.6%, respectively. Because this mutation results in a nearly complete loss of VWF-CP activity, we calculated that approximately 10% of the Japanese population has significantly reduced VWF-CP activity.

Discussion

In addition to the 12 reported mutations in the *ADAMTS13* gene (22), the present study identified three additional mutations responsible for reduced VWF-CP activity. All 15 mutations were excluded as common polymorphisms by the screening of a large panel of unaffected subjects. The mutated sites were not restricted to specific domains but located throughout the molecule. Some mutations such as R268P and C508Y would affect proper folding and secretion of VWF-CP, whereas some likely affect enzymatic activity.

This study and Levy *et al.* (22) identified eight missense common SNPs, R7W, Q448E, P475S, P618A, R625H, A732V, A900V, and A1033T. We demonstrated that the P475S mutation leads to dramatic decreases in VWF-CP activity, whereas Q448E has no effect. At present, P475S is the only common SNP associated with changes in VWF-CP activity. The functional importance of the remaining SNPs, if any, remains to be uncovered.

Although both the USS proband and his father in family A were compound heterozygotes, R268P/C508Y and R268P/P475S, respectively, only the proband was symptomatic (Fig. 1).

This finding may result from a differential effect between the C508Y and P475S mutations; the C508Y mutant was not secreted, whereas the P475S mutant was secreted normally and showed low but significant activity (Figs. 2 and 4). In 364 Japanese subjects we analyzed, one individual was homozygous for the P475S mutation, but was asymptomatic. This observation suggests that faint activity of VWF-CP is sufficient for normal hemostasis, consistent with reports (4, 13). Another homozygous mutation, Q449stop, was present in the USS proband of family B. At least in our expression system using HeLa cells, the recombinant Q449stop mutant was secreted from cells but possessed lower enzymatic activity than P475S. The subtle difference in activity may be critical for the onset of neonatal TTP. Alternatively, the absence of the Cys-rich, TSP1, and CUB domains in the Q449stop mutant may mediate the symptomatic difference. These strict correlations between mutation and phenotype may be partly true, especially in neonatal USS. However, much variation exists in the clinical phenotype of TTP, such as the age of onset and severity of symptoms. Therefore, the possibility cannot be excluded that additional genetic or nongenetic factors may also influence the occurrence of congenital TTP.

The P475S allelic frequency of 5.1% was determined from the analysis of 364 individuals. Although none of these patients demonstrated any symptoms of TTP, they were all patients of the Division of Hypertension and Nephrology at the National Cardiovascular Center (Suita, Japan). Therefore, the bias of this population may affect the allelic frequency. Further analysis will be required to determine the relationship between this SNP and hypertension or other related diseases.

A major proportion of TTP cases are not congenital but are acquired in adults possessing underlying conditions, including autoimmunity, pregnancy, and preexisting infection (2, 3, 31). Occasionally, severe TTP is induced as a side effect of drugs such as cyclosporine, ticlopidine, and clopidogrel (32–34). If the occurrence is associated with a particular genetic background, such as P475S polymorphism, genotyping before medication will be useful to prevent the development of drug-associated TTP.

We here demonstrate that some mutants, including Q449stop and P475S, are secreted from cells at levels similar to the WT VWF-CP. This observation suggests that the clinical assay based on the plasma VWF-CP activity is a more accurate prognostic test than the measurement of antigen levels to determine the VWF-CP-dependent hemostatic conditions of patients. Because current methods measuring VWF-CP activity require time and skill, they are not suitable for high-throughput screening. It will be important in the future to develop more rapid, accurate methods to assay VWF-CP activity in contrast to antigen levels.

We thank Ms. Yuko Nobe and Akemi Fukumoto (National Cardiovascular Center Research Institute) and Noriko Mimura (The Chemo-Sero-Therapeutic Research Institute) for their technical assistance. This work was supported in part by grants-in-aid from the Ministry of Health, Labor, and Welfare of Japan; the Ministry of Education, Culture, Sports, Science, and Technology of Japan; the Japan Society for the Promotion of Science; and the Program for Promotion of Fundamental Studies in Health Sciences of the Organization for Pharmaceutical Safety and Research of Japan.

1. Moschcowitz, E. (1924) *Proc. N. Y. Pathol. Soc.* **24**, 21–24.
2. Kakishita, E. (2000) *Int. J. Hematol.* **71**, 320–327.
3. Cines, D. B., Konkle, B. A. & Furlan, M. (2000) *Thromb. Haemostasis* **84**, 528–535.
4. Furlan, M. & Lämmle, B. (2001) *Best Pract. Res. Clin. Haematol.* **14**, 437–454.
5. Kinoshita, S., Yoshioka, A., Park, Y. D., Ishizashi, H., Konno, M., Funato, M., Matsui, T., Titani, K., Yagi, H., Matsumoto, M. & Fujimura, Y. (2001) *Int. J. Hematol.* **74**, 101–108.
6. Fujimura, Y., Matsumoto, M., Yagi, H., Yoshioka, A., Matsui, T. & Titani, K. (2002) *Int. J. Hematol.* **75**, 25–34.
7. Fujimura, Y. & Titani, K. (1994) in *Haemostasis and Thrombosis,* eds. Bloom, A. L., Forbes, C. D., Thomas, D. P. & Tuddenham, E. G. D. (Churchill Livingstone, New York), pp. 379–395.
8. Furlan, M. (1996) *Ann. Hematol.* **72**, 341–348.
9. Ruggeri, Z. M. (1997) *J. Clin. Invest.* **99**, 559–564.
10. Sadler, J. E. (1998) *Annu. Rev. Biochem.* **67**, 395–424.
11. Federici, A. B., Bader, R., Pagani, S., Colibretti, M. L., De Marco, L. & Mannucci, P. M. (1989) *Br. J. Haematol.* **73**, 93–99.
12. Kalafatis, M., Takahashi, Y., Girma, J. P. & Meyer, D. (1987) *Blood* **70**, 1577–1583.
13. Yagi, H., Konno, M., Kinoshita, S., Matsumoto, M., Ishizashi, H., Matsui, T., Titani, K. & Fujimura, Y. (2001) *Br. J. Haematol.* **115**, 991–997.
14. Furlan, M., Robles, R. & Lämmle, B. (1996) *Blood* **87**, 4223–4234.
15. Tsai, H. M. (1996) *Blood* **87**, 4235–4244.
16. Dent, J. A., Berkowitz, S. D., Ware, J., Kasper, C. K. & Ruggeri, Z. M. (1990) *Proc. Natl. Acad. Sci. USA* **87**, 6306–6310.
17. Tsai, H. M., Sussman, I. I. & Nagel, R. L. (1994) *Blood* **83**, 2171–2179.
18. Soejima, K., Mimura, N., Hirashima, M., Maeda, H., Hamamoto, T., Nakagaki, T. & Nozaki, C. (2001) *J. Biochem. (Tokyo)* **130**, 475–480.
19. Gerritsen, H. E., Robles, R., Lämmle, B. & Furlan, M. (2001) *Blood* **98**, 1654–1661.
20. Fujikawa, K., Suzuki, H., McMullen, B. & Chung, D. (2001) *Blood* **98**, 1662–1666.
21. Zheng, X., Chung, D., Takayama, T. K., Majerus, E. M., Sadler, J. E. & Fujikawa, K. (2001) *J. Biol. Chem.* **276**, 41059–41063.
22. Levy, G. G., Nichols, W. C., Lian, E. C., Foroud, T., McClintick, J. N., McGee, B. M., Yang, A. Y., Siemieniak, D. R., Stark, K. R., Gruppo, R., *et al.* (2001) *Nature (London)* **413**, 488–494.
23. Tang, B. L. & Hong, W. (1999) *FEBS Lett.* **445**, 223–225.
24. Hurskainen, T. L., Hirohata, S., Seldin, M. F. & Apte, S. S. (1999) *J. Biol. Chem.* **274**, 25555–25563.
25. Cal, S., Obaya, A. J., Llamazares, M., Garabaya, C., Quesada, V. & López-Otín, C. (2002) *Gene* **283**, 49–62.
26. Colige, A., Vandenberghe, I., Thiry, M., Lambert, C. A., Van Beeumen, J., Li, S. W., Prockop, D. J., Lapière, C. M. & Nusgens, B. V. (2002) *J. Biol. Chem.* **277**, 5756–5766.
27. Bork, P. & Beckmann, G. (1993) *J. Mol. Biol.* **231**, 539–545.
28. Niwa, H., Yamamura, K. & Miyazaki, J. (1991) *Gene* **108**, 193–199.
29. Furlan, M., Robles, R., Solenthaler, M., Wassmer, M., Sandoz, P. & Lämmle, B. (1997) *Blood* **89**, 3097–3103.
30. Mori, Y., Wada, H., Gabazza, E. C., Minami, N., Nobori, T., Shiku, H., Yagi, H., Ishizashi, H., Matsumoto, M. & Fujimura, Y. (2002) *Transfusion* **42**, 572–580.
31. Bell, W. R. (1997) *Semin. Hematol.* **34**, 134–139.
32. Sugio, Y., Okamura, T., Shimoda, K., Matsumoto, M., Yagi, H., Ishizashi, H., Niho, Y., Inaba, S. & Fujimura, Y. (2001) *Int. J. Hematol.* **74**, 347–351.
33. Reichenberger, F., Wirtz, H. & Paschke, R. (2001) *Cardiology* **96**, 51–52.
34. Medina, P. J., Sipols, J. M. & George, J. N. (2001) *Curr. Opin. Hematol.* **8**, 286–293.

Original Article

Aldehyde Dehydrogenase 2 Gene Is a Risk Factor for Myocardial Infarction in Japanese Men

Shuichi TAKAGI, Naoharu IWAI, Ryoko YAMAUCHI, Sunao KOJIMA, Shinji YASUNO, Takeshi BABA, Masahiro TERASHIMA, Yoshiaki TSUTSUMI, Shoji SUZUKI, Isao MORII, Sotaro HANAI, Koh ONO, Shunroku BABA, Hitonobu TOMOIKE, Atsushi KAWAMURA, Shunichi MIYAZAKI, Hiroshi NONOGI, and Yoichi GOTO

In epidemiological studies, moderate alcohol consumption has been consistently associated with a reduced risk of myocardial infarction (MI). About half of Japanese show an extremely high sensitivity to alcohol (ethanol), which is due to a missense mutation from glutamic acid (Glu) to lysine (Lys) at codon 487 in an isoenzyme of aldehyde dehydrogenase (ALDH2) with a low K_m. We obtained a preliminary result that subjects homozygous for the Lys 487 allele had higher risk for myocardial infarction. The purpose of the present study was to assess this hypothesis by employing a larger cohort of subjects with MI. The experimental group consisted of 342 male subjects with demonstrated MI who were selected randomly from our outpatient clinic. As controls, we employed 1,820 male subjects with no cardiovascular complications who were selected from the Suita Study. All subjects provided their written informed consent to participate in the genetic analyses. Subjects with MI were older and had higher body mass index, higher prevalence of diabetes mellitus, higher prevalence of smoking habit, higher prevalence of the Lys/Lys genotype (homozygous for Lys 487 allele), and lower high density lipoprotein (HDL) cholesterol level (HDL-C). The ALDH2 genotype affected the level of alcohol consumption, and HDL-C. Multiple logistic analyses indicated that the odds ratio of the Lys/Lys genotype to the Lys/Glu+Glu/Glu genotype was 1.56 (p=0.0359). Inclusion of HDL-C as one of the independent variables downplayed the importance of the ALDH2 genotype. This may indicate that the ALDH2 genotype affects MI *via* its effects on HDL-C. In conclusion, the ALDH2 Lys/Lys genotype is a risk factor for myocardial infarction in Japanese men due to its influence on HDL cholesterol level.
(*Hypertens Res* 2002; 25: 677–681)

***Key Words*: alcohol, genetics, myocardial infarction, aldehyde dehydrogenase 2, high density lipoprotein cholesterol**

Introduction

In epidemiological studies, moderate consumption of alcohol has been consistently associated with a reduced risk of myocardial infarction (*1–4*). The mechanisms underlying this association have not been fully clarified, but may include the effect of alcohol on high density lipoprotein (HDL) cholesterol level (*1, 2*). About half of Japanese show an extremely high sensitivity to alcohol (ethanol), which is due to a missense mutation from glutamic acid (Glu) to lysine (Lys) at codon 487 in an isoenzyme of aldehyde dehydrogenase

From the Division of Cardiology, National Cardiovascular Center, Suita, Japan.

This study was supported by the Program for Promotion of Fundamental Studies in Health Science of the Organization for Pharmaceutical Safety and Research of Japan.

Address for Reprints: Naoharu Iwai, M.D., Ph.D., Research Institute, National Cardiovascular Center, 5–7–1 Fujishirodai, Suita 565–8565, Japan. E-mail: niwai@res.ncvc.go.jp

Received March 4, 2002; Accepted in revised form May 7, 2002.

Table 1. Characteristics of the Study Population

	Control	MI	*p* value
N	1,820	342	
ALDH2	159/786/875	43/139/160	0.0792
Age	60.6 (0.3)	63.7 (0.6)	<0.001
BMI	23.0 (0.06)	23.7 (0.2)	0.0003
Alcohol	0.84 (0.02)	0.78 (0.05)	n.s.
%smoker	40.0	67.4	<0.001
%HT	39.2	55.8	<0.001
%DM	21.2	43.9	<0.001
HbA1c	5.4 (0.03)	5.7 (0.06)	<0.001
FBS	101 (0.6)	117 (1.5)	<0.001
Chol	203 (0.8)	201 (1.8)	n.s.
Trigly	143 (2.5)	142 (5.7)	n.s.
HDL	55 (0.3)	42 (0.8)	<0.001

Values are expressed as the mean±SE. *N*, number of subjects; MI, patients with myocardial infarction; ALDH2, number of subjects according to ALDH2 genotype (Lys/Lys, Lys/Glu, Glu/Glu); Age, years old; BMI, body mass index (kg/m^2); Alcohol, alcohol consumption in cups/day (one cup of Japanese alcohol corresponds to 25.2 ml ethanol); %smoker, percentage of subjects with a smoking habit; %HTN, percentage of subjects with hypertension; %DM, percentage of subjects with diabetes mellitus; HbA1c, shown as %; FBS, fasting blood sugar (mg/dl); Chol, cholesterol (mg/dl); Trigly, triglycerides (mg/dl); HDL, HDL cholesterol (mg/dl).

(ALDH2) with a low K_m. Thus, in Japanese, the level of alcohol consumption, and therefore the level of HDL cholesterol, are greatly influenced by the genotype of ALDH2 (*5–9*). In our previous study, we obtained a preliminary result that the ALDH2 Lys/Lys genotype (homozygous for the Lys 487 allele), which is associated with a lower metabolic rate of acetaldehyde, seems to be a risk factor for myocardial infarction (*9*). The purpose of the present study was to assess this hypothesis by employing a greater number of subjects with myocardial infarction.

Materials and Methods

Subjects

Control subjects were derived from the Suita Study (*9*, *10*). The selection criteria and design of the Suita Study have been described previously (*11*). The sample consisted of 14,200 men and women aged 30 to 79 years, stratified by sex and 10-year age groups, who were selected randomly from the municipal population registry. All subjects in the sample were sent a letter inviting them to attend a series of regular follow-up examinations (*i.e.*, one examination every 2 years). The basic sampling of the population started in 1989 with a cohort study base, and 51.7% (n=7,347) of the subjects responded to the invitation letter and had paid their initial visit to the National Cardiovascular Center by February, 1997. The participants visited the National Cardiovascular Center every 2 years for regular health check-ups. For the present study, we selected only male subjects without any cardiovascular complications (control group: n=1,820). The study group consisted of male subjects with documented myocardial infarction who were selected randomly from our outpatient clinic and met the following criteria: 1) chest pain of ≧30 min duration; 2) electrocardiographic ST segment elevation of ≧0.1 mV in two or more leads in the same vascular territory; and 3) subsequent elevation of creatine phosphokinase levels to more than twice the normal range (n=342). All subjects provided their written informed consent to participate in the genetic analyses. The present study was approved by the Committee on Genetic Analysis and Genetic Therapy of the National Cardiovascular Center.

DNA Studies

The ALDH2 genotype was determined by the TaqMan method as previously reported (*9*, *10*). Ten nanograms of sample DNA was amplified by PCR according to the manufacturer's recommendations (PE Applied Biosystems, Foster City, USA). The sense and antisense PCR primers and probes for Glu and Lys at codon 487 were as follows:
Sense primer: 5′-gtcaactgctatgatgtgtttgg-3′
Antisense primer: 5′-ccaccagcagaccctcaag-3′
Probe for Glu: Tet-gcaggcatacactgaagtgaaaactgtg
Probe for Lys: Fam-tgcaggcatacactaaagtgaaaactgtg

The genotypes corresponding to homozygosity for the Lys 487 allele, heterozygosity for the Lys 487 allele, and homozygosity for the Glu 487 allele were described as Lys/Lys, Lys/Glu, and Glu/Glu, respectively.

Statistical Analysis

Values are expressed as the mean±SE. All statistical analyses were performed using the JMP and StatView statistical software packages (SAS Inst. Inc., Cary, USA). Multiple linear regression and multiple logistic analyses were performed with other covariates. Differences in numerical data among the groups were analyzed by one-way/two-way analysis of variance (ANOVA) and unpaired Student's *t*-test. Differences in frequencies among the groups were tested by contingency table analysis. In multivariate analyses, genotypes of ALDH2 were categorized into two groups, namely Lys/Lys and Lys/Glu+Glu/Glu. Sample power calculation was performed using SPSS software (SPSS Inc., Chicago, USA).

Results

Subject Characteristics

Table 1 shows the characteristics of the study population.

Table 2. Relationship between Characteristics and ALDH2 Phenotype

	Lys/Lys	Lys/Glu	Glu/Glu	*p* value
N	202	925	1,035	
MI	43	139	160	0.0792
%MI	21.3	15.0	15.5	
Age	61.3 (0.8)	61.5 (0.4)	60.6 (0.4)	n.s.
BMI	23.1 (0.2)	23.0 (0.1)	23.3 (0.1)	n.s.
Alcohol	0.21 (0.06)	0.6 (0.03)	1.16 (0.03)	<0.0001
%smoker	48.5	47.9	47.7	n.s.
%HTN	40.6	37.7	46.9	0.0002
%DM	22.8	26.6	23.5	n.s.
HbA1c	5.5 (0.09)	5.6 (0.04)	5.5 (0.04)	n.s.
FBS	103 (2.0)	102 (0.9)	105 (0.9)	0.0397
Chol	203 (2.3)	203 (1.1)	203 (1.0)	n.s.
Trigly	134 (7.4)	137 (3.5)	150 (3.3)	0.0121
HDL	48 (1.0)	52 (0.5)	54 (0.5)	<0.0001

Values are expressed as the mean±SE. *N*, number of subjects according to ALDH2 genotype (Lys/Lys, Lys/Glu, Glu/Glu); MI, patients with myocardial infarction; Age, years old; BMI, body mass index (kg/m^2); Alcohol, alcohol consumption in cups/day (one cup of Japanese alcohol corresponds to 25.2 ml ethanol); %smoker, percentage of subjects with a smoking habit; %HTN, percentage of subjects with hypertension; %DM, percentage of subjects with diabetes mellitus; HbA1c, shown as %; FBS, fasting blood sugar (mg/dl); Chol, cholesterol (mg/dl); Trigly, triglycerides (mg/dl); HDL, HDL cholesterol (mg/dl).

Table 3. Multiple Logistic Analyses

	Odds ratio	*p*
A. Multiple logistic analyses		
ALDH2	1.56 (1.022–2.35)	0.0359
Smoker	16.51 (11.51–24.36)	<0.0001
DM	2.28 (1.735–2.998)	<0.0001
B. Multiple logistic analyses including HDL cholesterol		
ALDH2	1.13 (0.707–1.795)	0.5926
Smoker	11.9 (8.083–18.048)	<0.0001
DM	2.13 (1.563–2.890)	<0.0001

ALDH2: in multivariate analyses genotypes of ALDH2 were categorized into two groups, namely Lys/Lys and Lys/Glu+Glu/Glu. Smoker, subjects with smoking habit; DM, presence of diabetes mellitus.

Table 4. Multiple Logistic Analyses in Younger Subjects

	Odds ratio	*p*
A. Multiple logistic analyses in younger subjects (<60 years old)		
ALDH2	2.01 (1.154–3.443)	0.012
Smoker	18.64 (10.89–34.53)	<0.0001
DM	2.70 (1.862–3.909)	<0.0001
B. Multiple logistic analyses in younger subjects (<60 years old) including HDL cholesterol		
ALDH2	1.36 (0.720–2.497)	0.3364
Smoker	12.7 (7.139–24.340)	<0.0001
DM	2.17 (1.414–3.312)	0.0004

ALDH2: in multivariate analyses genotypes of ALDH2 were categorized into two groups, namely Lys/Lys and Lys/Glu+Glu/Glu. Smoker, subjects with smoking habit; DM, presence of diabetes mellitus.

Subjects with myocardial infarction were older, had higher blood sugar and HbA1c levels, lower HDL cholesterol level, higher body mass index (BMI), higher prevalence of diabetes mellitus (DM), higher prevalence of smoking habit, higher prevalence of hypertension and a higher prevalence of the ALDH2 Lys/Lys genotype.

Significance of the ALDH2 Genotype in Myocardial Infarction

Table 2 shows characteristics of subjects according to the ALDH2 genotype. The ALDH2 genotype affected the level of alcohol consumption, triglyceride level, HDL cholesterol level, blood sugar level and prevalence of hypertension.

The prevalence of subjects with myocardial infarction tended to be higher in subjects with the ALDH2 Lys/Lys genotype ($p=0.0792$, chi-squared test). Multiple logistic analyses indicated that the odds ratio of the risk of myocardial infarction for the Lys/Lys genotype compared with the Lys/Glu+Glu/Glu genotypes was 1.56 ($p=0.0359$; 95% confidence interval (CI): 1.02–2.35; Table 3A). Other variables were age ($p<0.0001$), BMI ($p<0.0001$), smoking habit ($p<0.0001$) and DM ($p<0.0001$) (Table 3A). Inclusion of HDL cholesterol as one of the independent variables downplayed the importance of the ALDH2 genotype ($p=0.5926$; 95% CI: 0.71–1.80; Table 3B). *P*-values for age, HDL cholesterol and BMI were <0.0001, <0.0001 and 0.1399, respectively. The association of the ALDH2 Lys/Lys genotype with myocardial infarction was more evi-

Table 5. Determinants of HDL Cholesterol

	p
A. Determinants of HDL cholesterol	
ALDH2	<0.0001
Smoker	<0.0001
DM	0.0022
B. Determinants of HDL cholesterol including alcohol consumption	
ALDH2	0.0014
Smoker	<0.0001
DM	0.0070
Alcohol	<0.0001

ALDH2: in multivariate analyses genotypes of ALDH2 were categorized into two groups, namely Lys/Lys and Lys/Glu+Glu/Glu. Smoker, subjects with smoking habit; DM, presence of diabetes mellitus; Alcohol, alcohol consumption.

dent in younger subjects (<60 years old). Multiple logistic analysis indicated that the odds ratio of the Lys/Lys genotype to the Lys/Glu+Glu/Glu genotypes was 2.01 (p=0.0120; 95% CI: 1.15–3.44; Table 4A). Other variables were age (p<0.0001), BMI (p=0.0006), smoking habit (p<0.0001) and DM (p<0.0001) (Table 4A). Again, inclusion of HDL cholesterol as one of the independent variables downplayed the importance of the ALDH2 genotype (p=0.3364; 95% CI: 0.72–2.50; Table 4B). *P*-values of age, HDL cholesterol and BMI were <0.0001, <0.0001 and 0.7142, respectively. These results suggest that the ALDH2 genotype may affect myocardial infarction by affecting HDL cholesterol.

Determinants of HDL Cholesterol

Multiple regression analysis indicated that the level of HDL cholesterol was determined by the ALDH2 genotype (Lys/Lys=1, Lys/Glu+Glu/Glu=2), presence of DM, and presence of smoking habit (Table 5A). Inclusion of alcohol consumption as one of the independent variables downplayed the importance of the ALDH2 genotype.

Sample Power Calculation

The sample power calculation in the present study indicated that sample power was 0.59 for the distribution, sample size and α value (0.05, two-tailed).

Discussion

Light-to-moderate consumption of alcohol has been consistently associated with a reduced risk of myocardial infarction (*1–4*). Heavier alcohol consumption, in contrast, is associated with no change or even an increase in this risk (*2*). The mechanisms underlying the former, beneficial association have not been fully clarified, but may include the effect of alcohol on HDL cholesterol level (*1, 2, 12–14*). Recently, Hines *et al.* reported that moderate drinkers who are homozygous for the slow-oxidizing alcohol dehydrogenase 3 (ADH3) allele ($\gamma 2\gamma 2$) have higher HDL cholesterol levels and a substantially decreased risk of myocardial infarction (*1*). Since the predominant function of ADH3 is to metabolize ethanol to acetaldehyde, they suggested that a slower rate of clearance of ethanol enhances the beneficial effect of moderate alcohol consumption on the risk of cardiovascular disease. In the present study, we showed that subjects who were homozygous for the Lys allele of ALDH2 had lower HDL cholesterol levels and a substantially increased risk of myocardial infarction. Since the ALDH2 enzyme metabolizes acetaldehyde to acetic acid, individuals with the Lys allele of ALDH2, which is associated with a lower metabolic rate of acetaldehyde, can tolerate only very small amounts of alcohol. The determinants of HDL cholesterol were the ALDH2 genotype (Lys/Lys=1, Lys/Glu+Glu/Glu=2), presence of DM, and presence of smoking habit. However, inclusion of alcohol consumption as one of the independent variables downplayed the importance of the ALDH2 genotype. Thus, since alcohol consumption determined by the ALDH2 genotype affects HDL cholesterol level, we emphasized the importance of the ALDH2 genotype for risk of myocardial infarction (*8, 9*).

De Oliveira e Silva *et al.* reported the mechanism of the effect of alcohol on HDL cholesterol level. They demonstrated that ethanol intake results in dose-dependent increases in plasma concentrations of the major HDL components (HDL cholesterol, apolipoproteins A-I and -II (apoA-I and -II) through an increase in the HDL apolipoprotein transport rate without a change in fractional catabolic rate or HDL particle size (*12*). However, the molecular mechanism of the increased apolipoprotein synthesis is unclear in humans *in vivo*. In hepatocyte culture, the effect of ethanol on apolipoprotein synthesis appears to involve the microsomal ethanol-oxidizing system and is speculated to be due to intracellular increases in phospholipid and cholesterol (*15, 16*).

We have previously assessed the significance of genetic polymorphisms of angiotensin converting enzyme (I/D), endothelial nitric oxide synthase (T(−788)C) and ABCA1 genes in ischemic heart disease using the same study population (*10, 17*). Our results indicated that these polymorphisms were not associated with ischemic heart disease in our study population, a finding that was discrepant with those of other previous studies (*18–20*). We have frequently encountered such discrepancy among association studies (*21–28*). The reason for the discrepancy is unclear, but it may be related to low statistical power or to differences among the ethnic groups studied.

The sample power was 0.59 in the present study, meaning that 59% of studies would be expected to yield a significant effect, rejecting the null hypothesis that the odds ratio is 1.0. To increase the sample power, additional studies employing larger cohorts will be needed.

References

1. Hines LM, Stampfer MJ, Ma J, *et al*: Genetic variation in alcohol dehydrogenase and the beneficial effect of moderate alcohol consumption on myocardial infarction. *N Engl J Med* 2001; **344**: 549–555.
2. Mukamal KJ, Jadhav PP, D'Agostino RB, *et al*: Alcohol consumption and hemostatic factors: analysis of the Framingham Offspring Cohort. *Circulation* 2001; **104**: 1367–1373.
3. Gaziano JM, Buring JE, Breslow JL, *et al*: Moderate alcohol intake, increased levels of high-density lipoprotein and its subfractions, and decreased risk of myocardial infarction. *N Engl J Med* 1993; **329**: 1829–1834.
4. Gaziano JM, Gaziano TA, Glynn RJ, *et al*: Light-to-moderate alcohol consumption and mortality in the Physicians' Health Study enrollment cohort. *J Am Coll Cardiol* 2000; **35**: 96–105.
5. Shibuya A, Yoshida A: Frequency of atypical aldehyde dehydrogenase-2 gene in Japanese and Caucasians. *Am J Hum Genet* 1988; **43**: 741–743.
6. Ikawa M, Impraim CC, Wang G, Yoshida A: Isolation and characterization of aldehyde dehydrogenase isoenzyme from usual and atypical human liver. *J Biol Chem* 1983; **258**: 6282–6287.
7. Yoshida A, Huang IY, Ikawa M: Molecular abnormality of an inactive aldehyde dehydrogenase variant commonly found in Orientals. *Proc Natl Acad Sci USA* 1984; **81**: 258–261.
8. Okayama A, Ueshima H, Yamakawa M, Kita Y: Low-K_m aldehyde dehydrogenase deficiency does not influence the elevation of blood pressure by alcohol. *J Hum Hypertens* 1994; **8**: 205–208.
9. Takagi S, Baba S, Mannami T, *et al*: The aldehyde dehydrogenase 2 gene is a risk factor for hypertension in Japanese but not alter the sensitivity to pressor effects of alcohol. *Hypertens Res* 2001; **24**: 365–370.
10. Takagi S, Iwai N, Goto Y, Nonogi H, Baba S: Genetic polymorphisms of angiotensin converting enzyme (I/D) and endothelial nitric oxide synthase (T(−788)C) genes in Japanese patients with myocardial infarction. *Thromb Haemost* 2001; **86**: 1339–1340.
11. Tsujita Y, Iwai N, Katsuya T, *et al*: Lack of association between genetic polymorphism of *CYP11B2* and hypertension in Japanese: the Suita Study. *Hypertens Res* 2001; **24**: 105–109.
12. De Oliveira e Silva ER, Foster D, Harper MM, *et al*: Alcohol consumption raises HDL cholesterol levels by increasing the transport rate of apolipoproteins A-I and A-II. *Circulation* 2000; **102**: 2347–2352.
13. Fumeron F, Betoulle D, Luc G, *et al*: Alcohol intake modulates the effect of a polymorphism of the cholesteryl ester transfer protein gene on plasma high density lipoprotein and the risk of myocardial infarction. *J Clin Invest* 1995; **96**: 1664–1671.
14. Mayer EJ, Newman B, Quesenberry CP Jr, Friedman GD, Selby JV: Alcohol consumption and insulin concentrations: role of insulin in associations of alcohol intake with high-density lipoprotein cholesterol and triglycerides. *Circulation* 1993; **88**: 2190–2197.
15. Tam S-P: Effect of ethanol on lipoprotein secretion in two human hepatoma cell lines, Hep G2 and Hep 3B. *Alcohol Clin Exp Res* 1992; **16**: 1021–1028.
16. Dashti N, Franklin FA, Abrahamson DR: Effect of ethanol on the synthesis and secretion of Apo A-I and apo B-containing lipoproteins in Hep G2 cells. *J Lipid Res* 1996; **37**: 810–824.
17. Takagi S, Iwai N, Miyazaki S, Nonogi H, Goto Y: Relationship between ABCA1 genetic variation and HDL cholesterol level in subjects with ischemic heart disease in Japanese. *Thromb. Haemost* (in press).
18. Keavney B, McKenzie C, Parish S, *et al*: Large-scale test of hypothesised associations between the angiotensin-converting-enzyme insertion/deletion polymorphism and myocardial infarction in about 5000 cases and 6000 controls: International Studies of Infarct Survival (ISIS) Collaborators. *Lancet* 2000; **355**: 434–442.
19. Nakayama M, Yasue H, Yoshimura M, *et al*: $T^{786}\rightarrow C$ mutation in the 5′-flanking region of the endothelial nitric oxide synthase gene is associated with coronary spasm. *Circulation* 1999; **99**: 2864–2870.
20. Clee SM, Zwinderman AH, Engert JC, *et al*: Common genetic variation in ABCA1 is associated with altered lipoprotein levels and a modified risk for coronary artery disease. *Circulation* 2001; **103**: 1198–1205.
21. Yuxiao F, Katsuya T, Asai T, *et al*: Lack of correlation between Mbo I restriction fragment length polymorphism of rennin gene and essential hypertension in Japanese. *Hypertens Res* 2001; **24**: 295–298.
22. Sugiyama T, Kato N, Ishinaga Y, Yamori Y, Yazaki Y: Evaluation of selected polymorphisms of the mendelian hypertensive disease genes in the Japanese population. *Hypertens Res* 2001; **24**: 515–521.
23. Frossard PM, Lestringant GG, Elshahat YI, John A, Obineche EN: An MboI two-allele polymorphism may implicate the human renin gene in primary hypertension. *Hypertens Res* 1998; **21**: 221–225.
24. Okura T, Kitami Y, Hiwada K: Restriction fragment length polymorphisms of the human renin gene: association study with a family history of essential hypertension. *J Hum Hypertens* 1993; **7**: 457–461.
25. Mune T, Rogerson FM, Nikkila H, Agarwal AK, White PC: Human hypertension caused by mutations in the kidney isozyme of 11 beta-hydroxysteroid dehydrogenase. *Nat Genet* 1995; **10**: 394–399.
26. Geller DS, Farhi A, Pinkerton N, *et al*: Activating mineralocorticoid receptor mutation in hypertension exacerbated by pregnancy. *Science* 2000; **289**: 119–123.
27. Baker EH, Dong YB, Sagnella GA, *et al*: Association of hypertension with T594M mutation in beta subunit of epithelial sodium channels in black people resident in London. *Lancet* 1998; **351**: 1388–1392.
28. Ambrosius WT, Bloem LJ, Zhou L, *et al*: Genetic variants in the epithelial sodium channel in relation to aldosterone and potassium excretion and risk for hypertension. *Hypertension* 1999; **34**: 631–637.

Predisposing factors for enlargement of intracerebral hemorrhage in patients treated with warfarin

Masahiro Yasaka, Kazuo Minematsu, Hiroaki Naritomi, Toshiyuki Sakata, Takenori Yamaguchi
Cerebrovascular Division, Department of Medicine, National Cardiovascular Center, Osaka, Japan

Summary
To elucidate predisposing factors for enlargement of intracerebral hematoma (ICH) during warfarin therapy, we reviewed 47 patients on warfarin who developed acute ICH and determined relationships among ICH enlargement, INR reversal and clinical data. Among 36 patients treated to counteract the effects of warfarin within 24 h of onset, ICH increased in 10 patients (enlarged group), but remained unchanged in the remaining 26 (unchanged group), while ICH remained unchanged in another 11 patients in whom the effect of warfarin was reversed after 24 h. The international normalized ratio (INR) was counteracted immediately in 11 patients treated with prothrombin complex concentrate (PCC) but gradually in the other 36 treated by reducing the dose of warfarin, or by administering vitamin K or fresh frozen plasma. Multivariate analysis with a logistic regression model showed an INR value <2.0 at admission or for 24 h after immediate INR correction with PCC prevented ICH enlargement (OR 0.069, 95%CI 0.006-0.789, p = 0.031). An INR value of >2.0 within 24 h of ICH seems an important predisposing factor for ICH enlargement.

Keywords
Intracerebral hematoma, warfarin, prothrombin complex concentrate, international normalized ratio

Thromb Haemost 2003; 89: 278–83

Introduction

Intracerebral hemorrhage (ICH) is one of the most serious hemorrhagic complications associated with warfarin treatment. The relative risk of ICH during oral anticoagulant therapy increases more than ten-fold in patients over 50 years of age (1). Bleeding is more protracted and hematomas are larger in patients treated with anticoagulants than in those with spontaneous ICH (2, 3). The annual risk of anticoagulant-related ICH is 1.1% per year among patients who have cerebrovascular disease and who are treated with anticoagulants (4). Hylek et al. reported that the risk of intracerebral and subdural hematoma significantly increases when the international normalized ratio (INR) value was above 4.0 (5). Yamaguchi et al. reported that the standard intensity of warfarin (INR 2.2–3.5) carried a higher risk of severe hemorrhagic complication than a lower intensity (INR 1.5–2.1) in elderly patients with non-valvular atrial fibrillation (NVAF) (6).

Our prior study revealed that the predisposing factors to hematoma growth among patients with spontaneous intracerebral hemorrhage were acute phase within 6 h of onset, hypertension, diabetes mellitus, liver diseases and a history of brain infarction (7). However, such factors in patients treated with warfarin have not been fully investigated.

The effect of warfarin can be counteracted by administering vitamin K or a combination of vitamin K and 800–1,000 ml of

Correspondence to:
Masahiro Yasaka, M.D.,
Cerebrovascular Division, Department of Medicine,
National Cardiovascular Center,
5-7-1 Fujishirodai, Suita, Osaka 565-8565, Japan
Tel.: +81-6-6833-5012, Fax: +81-6-6872-7486,
E-mail: yasakam@hsp.ncvc.go.jp or yasakam@gray.plala.or.jp

Received October 20, 2002
Accepted after revision December 6, 2002

fresh frozen plasma (FFP) depending on INR values, in addition to the discontinuation of warfarin. However, administration of FFP carries a risk of viral infection, requires long preparation time and often causes volume overload. These strategies may result in enlarged ICH accompanied by deteriorating neurological deficits or heart failure (8, 9). Prothrombin complex concentrate (PCC) has recently been introduced as an agent that can correct INR faster than FFP in warfarin-related coagulopathy (8-11). We have corrected high INR values using PCC since December 2000, because it counteracts the effects of warfarin within 10 minutes (12).

We examined the predisposing factors for ICH enlargement and determined whether PCC is useful to prevent it in patients treated with warfarin. We retrospectively investigated consecutive patients who developed acute ICH during warfarin treatment, from December 2000 to September 2002 when PCC was administered and from January 1992 to November 2000 when conventional treatment was applied.

Methods

We retrospectively reviewed the hospital records of 50 consecutive patients who developed ICH. These patients were admitted to our stroke care unit within five days of ICH onset and the diagnosis was confirmed by CT. Excluded from the study were three patients who were comatose upon admission and who died within three days of ICH onset due to brain herniation. We thus studied 47 patients (35 men and 12 women; median age, 69 [range 16–89] years) with acute ICH.

The primary underlying diseases requiring anticoagulation were NVAF in 22 patients, mitral or aortic valve replacement in 11, deep vein thrombosis in four, dilated cardiomyopathy in three, coronary artery bypass graft for ischemic heart disease in three, complicated atheromatous lesions at the aortic arch in two, and atherosclerotic obliterans and homograft-shunt operation for hemodialysis in one each. Twenty-four of the patients had a history of brain infarction.

The second CT examination was performed routinely within 24 h after starting treatment to counteract the warfarin effects and the third was implemented within a few days after that. An additional CT scan was also performed if a patient clinically deteriorated.

A parenchymal hematoma was located at the thalamus in 18 patients, the putamen in 8, the thalamus and putamen in one, the caudate head in two, the subcortex in 13, the cerebellum in four, and pons in one.

The volume of ICH was determined as follows (13). The longest diameter (A) and the largest diameter (B) perpendicular to A were measured using the centimeter scale on CT films of slices showing the largest area of ICH. The height of the hematoma (C) was calculated by multiplying the number of slices involved and slice thickness. Hemorrhage within the ventricular system was not measured. The three diameters were multiplied and then divided by two to obtain the volume of ICH ($A \times B \times C/2$) (10). When volume after treatment was 1.4-fold larger than that before, the parenchymal hemorrhage was considered to have enlarged.

The effects of warfarin were counteracted by stopping or reducing the amount of warfarin, administration of only vitamin K, or of fresh frozen plasma (FFP) with or without vitamin K, and 500–1,500 IU of prothrombin concentrate complex (PCC) with or without vitamin K. The effect on INR correction by each therapy was monitored by measuring INR more than twice from 10 min to 24 h after starting the treatment.

We determined relationships between ICH volume and age, gender, hypertension, diabetes mellitus, underlying disease for anticoagulation, liver disease, history of brain hemorrhage, antiplatelet medication, duration from ICH onset to commencement of treatment, INR, systolic blood pressure (SBP), and serum blood sugar level at the time of admission, as well as INR and SBP after the treatment.

Hypertension was defined as the use of antihypertensive agents or blood pressure with a systolic value of > or = 160 mmHg or a diastolic value of > or = 95 mmHg. Diabetes mellitus was defined as the use of insulin or oral hypoglycemic agents, fasting blood glucose levels of > or = 140 mg/dl, or random blood glucose levels of > or = 200 mg/dl. Liver disease was defined as a diagnosis of liver cirrhosis or active hepatitis.

Data are expressed as median and range. Univariate analyses were performed based on the Mann-Whitney U test, the chi square test, or Fisher's exact test for instances in which counts of individual cells in a 2×2 table were below five. We performed multivariate analyses with a logistic regression

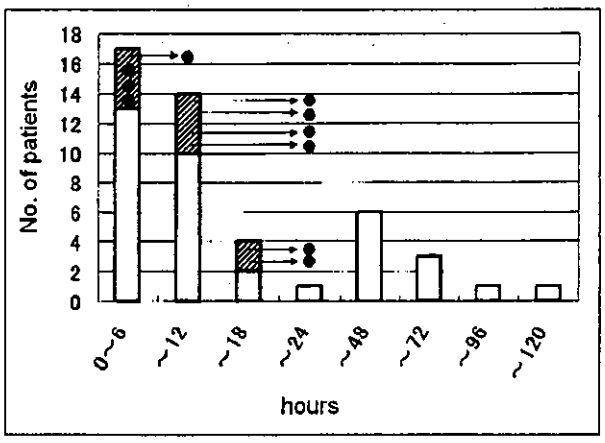

Figure 1: Number of patients with intracerebral hematoma during warfarin treatment stratified by time from onset to commencement of treatment, and by presence (shaded bar) or absence (white bar) of enlarged intracerebral hematoma. Closed circles indicate points in time when ICH enlargement was confirmed by CT

model using values of p <0.15 in univariate analyses. A p-value below 0.05 was considered significant, and values between 0.05 and 0.1 were considered marginally significant.

Results

Warfarin counteraction was commenced within 24 h of ICH onset in 36 patients and after 24 h in the remaining 11 patients. Among the 36 patients, ICH enlargement was confirmed in 10 (28%, enlarged group) but was not observed in the other 26 (unchanged group) and was definitely absent in the 11 patients who underwent treatment after 24 h of ICH (p = 0.0885). In four of the 17 patients in whom the treatment was commenced within six hours of onset, ICH enlarged, which was confirmed by CT within six hours in three patients and at six hours and a half in the other one (Fig. 1). In six of the 19 patients in whom the treatment was started between six and 24 h of onset, ICH enlargement occurred, which was confirmed by CT from 18 to 24 h after the onset of the ICH. Neurological deterioration was accompanied with eight of the ten patients with ICH enlargement (Fig. 2).

Patients tended to be younger (Mann-Whitney U test, p = 0.0961) and had liver diseases more frequently (Fisher's exact test, p = 0.0152) in the enlarged group than in the unchanged group (Table 1). Gender, history of hypertension, incidence of diabetes mellitus, hypercholesterolemia, ischemic stroke and brain hemorrhage did not significantly differ among the groups. Antiplatelet therapy accompanied warfarin administration in 20% of the enlarged group and in 35% of the unchanged group (p = 0.6880).

Although median ICH volume at the time of admission in the enlarged group was larger than that in the unchanged group,

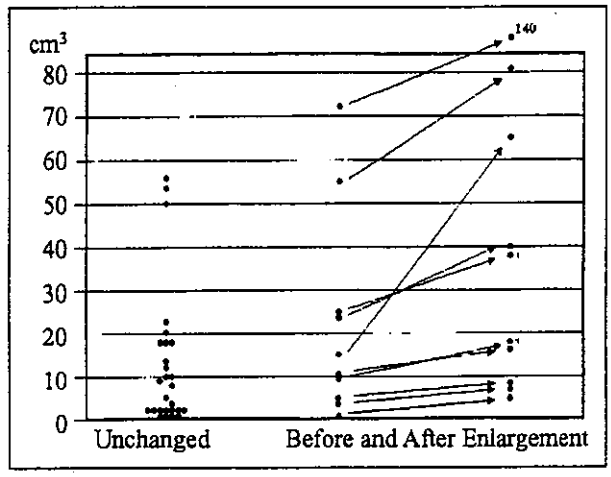

Figure 2: Hematoma volumes on admission in unchanged and enlarged groups, and those after enlargement in the latter group. * indicates patients without neurological deterioration.

it was not significant (Mann-Whitney U test, p = 0.1288, Fig. 2 and Table 2).

The INR values on admission in the enlarged group were always above 2.0, which were higher than those in the unchanged group with significance (Mann-Whitney U test, p = 0.0217) (Fig. 3 and Table 2).

Duration from the onset of ICH and commencement of treatment was 1-109 h (median 9 h). The numbers of cessations or reductions of warfarin (40% vs. 35%), administration of vitamin K (30% vs. 27%), or FFP (10% vs. 4%), or PCC (20% vs. 35%) did not significantly differ between the enlarged and unchanged groups (Table 3).

The INR levels in eleven patients treated with PCC was corrected from a median of 2.64 (2.26–10) to 1.14 (0.91-1.63)

	Enlarged n=10	Unchanged n=26	p value
Male	8 (80)	20 (77)	>0.9999
Age*	63 [46-74]	71 [16-83]	0.0961
Hypertension	9 (90)	20 (77)	0.6454
Diabetes Mellitus	3 (30)	7 (27)	>0.9999
Hypercholesterolemia	2(20)	3 (12)	0.6034
Ischemic stroke	6 (60)	13 (50)	0.7169
Brain hemorrhage	2 (20)	3 (12)	0.6034
Liver disease	4 (40)	1 (4)	0.0152
Antiplatelet therapy	2 (20)	9 (35)	0.6880

Table 1: Demographics of patients. *, Mann Whitney U test; without *, Chi square test; ( ), %; [ ], median and range.

Table 2: Clinical and laboratory data. SBP, systolic blood pressure; *, Mann Whitney U test; without *, Chi square test; ( ), % ; [ ], median and range; **, Number of patients with INR <2.0 at admission or rapid correction of INR with PCC and vitamin K.

	Enlarged n=10	Unchanged n=26	p value
At admission			
SBP (mmHg)*	161 [114-220]	162 [100-190]	0.7108
Blood sugar (mg/dl)*	160 [80-260]	125 [84-371]	0.1864
INR*	2.74 [2.1-10]	2.20 [1.11-4.0]	0.0217
INR >2.0	10(100)	17(65)	0.0394
Hematoma size (cm^2)*	12.2 [0.7-72]	6.0 [0.5-56]	0.1288
24 hours after treatment			
SBP (mmHg)*	150 [104-240]	142 [100-170]	0.9718
INR <2.0 **	1 (10)	18(69)	0.0023

10-60 minutes after an intravenous injection of PCC (500 IU in nine patients, 1,000 IU and 1,500 IU in one each) and a low INR level was maintained for at least 24 h in ten of them (Table 3). In the remaining patient, INR was decreased from 10.0 to 1.63 by 500 IU of PCC without vitamin K, but this value increased again to 2.60 and ICH enlarged 12 h after treatment. On the other hand, the amount of time required for INR values to decrease from > 2.0 to that between 1.2 and 1.9 was longer in patients treated without than with PCC.

The INR levels at admission were higher in the enlarged group than in the unchanged group (2.74 [2.1-10] vs. 2.20 [1.11-4.0], p = 0.0217, Table 2) and INR >2.0 at admission was more frequent in the enlarged group than in the unchanged group (100% vs. 65%, p = 0.0394, Fig. 3). The frequency of patients with INR <2.0 before treatment or for at least 24 h after PCC injection was significantly smaller in the enlarged group than in the unchanged group (10% vs. 69%, p = 0.0023).

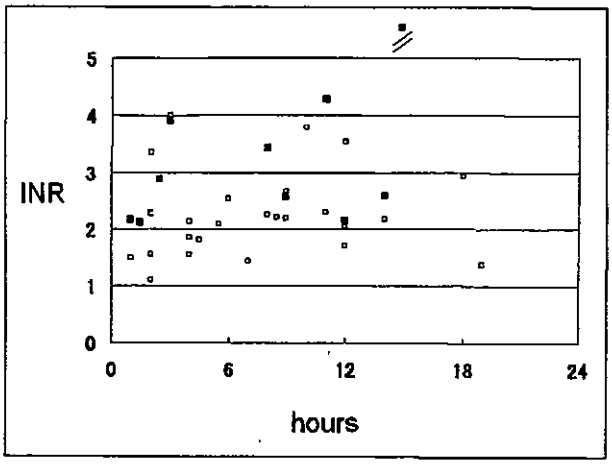

Figure 3: INR values on admission in patients admitted within the first 24 hours. Open squares, INR values of unchanged group; closed squares, INR values of enlarged group.

SBP and blood sugar at admission and SBP during the first 24 h after starting treatment did not significantly differ between the two groups (Table 2). The SBP was >200 mmHg at admission and during the 24 h after treatment in two patients of the enlarged group and in none of the unchanged group.

We selected the variables of liver disease, age, hematoma size and INR <2.0 before treatment or for at least 24 h after PCC injection as independent factors for multivariate analyses with a logistic regression model for hematoma enlargement. The analysis demonstrated that the INR <2.0 before treatment or for at least 24 h after PCC injection was significant (OR 0.069, 95%CI 0.006–0.789, p = 0.0312, Table 4).

Discussion

Although bleeding is more protracted and hematomas are larger in patients treated with warfarin than in those with spontaneous intracerebral hemorrhage (2, 3), the time window for ICH enlargement in patients treated with warfarin remains obscure. Fujii et al. retrospectively found enlarged hematomas in 14% of 627 patients with spontaneous intracerebral hemorrhage admitted within 24 h of onset (14). Kazui et al. reviewed the clinical records of 204 patients with spontaneous intracerebral hemorrhage and found enlarged hematomas in 41 (20%) of them within 24 h of onset in 34 (83%) of the 41 within 6 h and in 7 (17%) from 6 to 24 h (7). On the contrary, our study of patients treated with warfarin demonstrated a higher frequency of hematoma enlargement (28%). More than half of these

Table 3: Treatment to counteract warfarin and INR values. n*, Number of patients with available INR data; h, hours; min, minutes INR before, INR value before treatment; INR after, INR value after treatment.

	Enlarged	Unchanged	Adm. > 24 h	Total	n*	INR before		INR after		Duration	
						Median	Range	Median	Range	Median	Range
W	4	9	6	19	7	2.60	2.20-3.13	1.79	1.34-1.98	38 h	13-168 h
K	3	7	4	14	11	2.25	2.03-5.66	1.79	1.23-1.98	6 h	1-42 h
FFP	1	1	1	3	3	3.35	2.10-3.39	1.40	1.39-1.80	24 h	8-24 h
PCC	2	9	0	11	11	2.64	2.26- 10.0	1.14	0.91-1.63	10 min	10-60 min
Total	10	26	11	47							

enlargements (70%) were confirmed by CT between 6 and 24 h, but not thereafter. Therefore ICH patients treated with warfarin must be carefully monitored not only within six hours of onset but also within 24 h of onset. Although our subjects received treatment soon after admission, the period between ICH onset and the start of treatment was relatively long (median 9 h). To receive appropriate treatment to prevent ICH enlargement, patients should be educated about visiting an emergency hospital as soon as possible after stroke symptoms occur.

The size of small hematomas in patients with spontaneous intracerebral hemorrhage is unlikely to further increase (7). However, the present study found that 40% of the hematomas were smaller than 10 cm^2 on admission in the enlarged group. Therefore, the potential hazard of enlargement in patients treated with warfarin cannot be excluded, if a small hematoma is recognized within 24 h of ICH onset.

Our data showed that INR levels in the enlarged group were always above 2.0 and higher than those in the unchanged group. In addition, the number of patients with an INR value of <2.0 before treatment or for at least 24 h after immediate correction by PCC was significantly smaller in the enlarged group than in the unchanged group. Multivariate analyses with logistic regression model demonstrated that an INR value of <2.0 before treatment or for 24 h after PCC treatment is an independent factor that is negatively associated with ICH enlargement. Therefore, an INR value of ≥2.0 seems to be a predisposing factor for ICH enlargement. Rapid reversal of INR with PCC and vitamin K seems effective when INR at admission is above 2.0 and this may improve the outcome of patients with ICH.

Table 4: Logistic regression analysis for enlargement of hematoma. *, at admission or for 24 h after treatment with PCC and vitamin K.

Variable	OR	95%CI	P
INR <2.0 *	0.069	0.006 - 0.789	0.0312
Liver diseases	7.050	0.506 - 98.205	0.1461
Age	1.011	0.937 - 1.091	0.7736
Hematoma size	1.041	0.974 - 1.113	0.2340

Liver dysfunction can also affect the progression of ICH (7, 14, 15). Fujii and coauthors demonstrated that the incidence of hematoma enlargement significantly increases with the severity of liver dysfunction (14). Decreased levels of coagulant factors caused by both warfarin and liver disease may increase the risk of ICH enlargement.

Although SBP at admission and for 24 h after treatment did not differ between the enlarged and unchanged groups, SBP was >200 mmHg in only two of the enlarged group. Kazui et al. reported that an SBP value of > or = 200 mmHg was a predisposing factor to the enlargement of spontaneous intracerebral hemorrhage (7). Broderick and associates recorded an SBP value of > or = 195 mmHg during the first 6 h in 5 of 6 patients, whose neurological condition deteriorated with a >40% increase in hematoma volume (16). Hypertension is obvious in patients with active bleeding (17, 18). Controlling SBP below 200 mmHg may be helpful to prevent ICH enlargement during the acute phase.

In conclusion, the predisposing factors to enlargement of warfarin-related ICH appeared to be an INR value of >2.0 within 24 h of onset and the absence of rapid treatment to counteract INR. Because the present study was retrospective and the study populations were small, a prospective study should compare PCC with other conventional treatment modalities in a large number of patients.

Acknowledgements

Financial Support: This study was partially supported by the Japanese Ministry of Health, Labor and Welfare (12A-1 and 12C-2).

References

1. Winzen AR, de Jonge H, Loeliger EA, Bots GTAM. The risk of intracerebral hemorrhage during oral anticoagulant treatment: A population study. Ann Neurol 1984; 16: 553-8.
2. Kase CS, Robinson RK, Stein RW, DeWitt LD, Hier DB, Harp DL, Williams JP, Caplan LR, Mohr JP. Anticoagulant-related intracerebral hemorrhage. Neurology 1985; 35: 943-8.
3. Franke CL, de Jonge J, van Swieten JC, Op de Coul AAW, van Gijn J. Intracerebral hematomas during anticoagulant treatment. Stroke 1990; 21: 726-30.
4. Staaf G, Norrving B, Nilsson B. Intracerebral hematomas during anticoagulant treatment. Acta Neurol Scand 1987; 76: 391.
5. Hylek EM, Singer DE. Risk factors for intracranial haemorrhage in outpatients taking warfarin. Ann Intern Med 1994; 120: 897-902.
6. Yamaguchi T, for Japanese NVAF-Embolism Secondary Prevention Cooperative Study Group. Optimal intensity of warfarin therapy for secondary prevention of stroke in patients with nonvalvular atrial fibrillation. A multicenter prospective randomized trial. Stroke 2000; 31: 817-21.
7. Kazui S, Minematsu K, Yamamoto H, Sawada T, Yamaguchi T. Predisposing factors to enlargement of spontaneous intracerebral hematoma. Stroke 1997; 28: 2370-5.
8. Boulis NB, Bobek MP, Schmaier A, Hoff JT. Use of factor IX complex in warfarin-related intracranial hemorrhage. Neurosurgery 1999; 45: 1113-9.
9. Cartmill M, Dolan G, Byrne JL, Byrne PO. Prothrombin complex concentrate for oral anticoagulant reversal in neurosurgical emergency. Br J Neurosurg 2000; 14: 458-61.
10. Fredriksson K, Norrving B, Stromblad LG. Emergency reversal of anticoagulation after intracerebral hemorrhage. Stroke 1992; 23: 972-7.
11. Makris M, Graves M, Phillips WS, Kitchen S, Rosendaal FR. Emergency oral anticoagulant reversal: The relative efficacy of infusions of fresh frozen plasma and clotting factor concentrate on correction of the coagulopathy. Thromb Haemost 1997; 77: 477-80.
12. Yasaka M, Sakata T, Minematsu K, Naritomi H, Yamaguchi T. Effect of prothrombin complex concentrate on intracranial hemorrhage in patients with warfarin treatment [abstract]. Stroke 2002; 33: 379.
13. Kothari RU, Brott T, Broderick JP, Barsan WG, Sauerbeck LR, Zuccarello M, Khoury J. The ABCs of measuring intracerebral hemorrhage volume. Stroke 1996; 27: 1304–5.
14. Fujii Y, Tanaka R, Takeuchi S, Koike T, Minakawa T, Sasaki O. Hematoma enlargement in spontaneous intracerebral hemorrhage. J Neurosurg 1994; 80: 51–7.
15. Niizuma H, Shimizu Y, Nakasato N, Jokura H, Suzuki J. Influence of liver dysfunction on volume of putaminal hemorrhage. Stroke 1988; 19: 987–90.
16. Broderick JP, Brott TG, Tomsick T, Barsan W, Spilker J. Ultra-early evaluation of intracerebral hemorrhage. J Neurosurg 1990; 72: 195-9.
17. Kelly RE, Berger JR, Scheinberg P, Stokes N. Active bleeding in hypertensive intracerebral hemorrhage: computed tomography. Neurology 1982; 32: 852–6.
18. Chen ST, Chen SD, Hsu CY, Hogan EL. Progression of hypertensive intracerebral hemorrhage. Neurology 1989; 39: 1509–14.

ELSEVIER

Neuroscience Letters 341 (2003) 37–40

Neuroscience Letters

www.elsevier.com/locate/neulet

Post-ischemic cyclooxygenase-2 expression is regulated by the extent of cerebral blood flow reduction in non-human primates

Chiaki Yokota[a,*], Yuji Kuge[b,c], Hiroyasu Inoue[d], Masafumi Tagaya[e], Go Kito[f], Teruo Susumu[f], Nagara Tamaki[g], Kazuo Minematsu[h]

[a]*Cerebrovascular Laboratory, National Cardiovascular Center Research Institute, 5-7-1 Fujishirodai, Suita, 565-8565, Japan*
[b]*Department of Tracer Kinetics, Graduate School of Medicine, Hokkaido University, Nishi 7, Kita-15, Kita-ku, Sapporo, 060-8638, Japan*
[c]*Institute for Biofunctional Research Co., Inc, 5-7-1 Fujishirodai, Suita, 565-0873, Japan*
[d]*Division of Molecular Pharmacology, Department of Pharmacology, National Cardiovascular Center Research Institute, 5-7-1 Fujishirodai, Suita, 565-8565, Japan*
[e]*Department of Medicine, National Osaka Hospital, 2-1-14, Houenzaka, Chuoku, Osaka, 540-0006, Japan*
[f]*Shin Nippon Biomedical Laboratories, Ltd., 2438, Miyanoura, Yoshidacho, Kagoshima-gun, Kagoshima, 891-1305, Japan*
[g]*Department of Nuclear Medicine, Graduate School of Medicine, Hokkaido University, Nishi 7, Kita-15, Kita-ku, Sapporo, 060-8638, Japan*
[h]*Cerebrovascular Division, Department of Medicine, National Cardiovascular Center, 5-7-1 Fujishirodai, Suita, 565-8565, Japan*

Received 17 December 2002; received in revised form 22 January 2003; accepted 24 January 2003

Abstract

We determined whether up to 24 h of ischemia could induce the expression of cyclooxygenase-2 (COX-2) in the brain of nonhuman primates. Randomized animals were subjected to either a 2 h ischemia (group II; $n = 3$) or a 24 h ischemia (group III; $n = 3$). Three animals in group I served as controls. In group III, regional cerebral blood flow (CBF) and the cerebral glucose metabolic rate (CMRglc) were evaluated using positron emission tomography. Upregulation of COX-2 mRNA expression was observed after 2 h of ischemia, but disappeared by 24 h in the ischemic temporal cortex, in which both CMRglc and CBF were markedly reduced. In the ischemic parietal cortex, where CMRglc was preserved, COX-2 expression persisted even 24 h after ischemia. This study is the first to demonstrate neuronal COX-2 induction within potentially viable hypoperfused brain areas in nonhuman primates.

Keywords: Cyclooxygenase-2; Focal brain ischemia; Positron emission tomography; Primate; Cerebral blood flow; Cerebral glucose metabolic rate

Cyclooxygenase-2 (COX-2) is expressed in the brain in discrete neuronal populations in the cortex in response to activation of *N*-methyl-D-aspartate (NMDA) receptors [13]. Several reports, using various rodent models, suggested that COX-2 played role in the development of ischemic injury during focal brain ischemia [1,10]. Supporting these data are the findings in COX-2 deficient mice of a significant reduction in brain injury that was produced by occlusion of the middle cerebral artery, compared to control animals [4]. While these data support the notion that COX-2 inhibition might represent a possible therapeutic target for ischemic stroke, it is still not clear from the few postmortem studies that have been reported [3,11], whether COX-2 is expressed during the acute phase of a stroke. To begin to address this question, we developed a primate model of thromboembolic stroke [7] in which we measured serial changes in cerebral blood flow (CBF) before and after arterial occlusion using positron emission tomography (PET) [8]. The temporal cortex and basal ganglia ipsilateral to the arterial embolization were regarded as the ischemic core, while the ipsilateral parietal cortex was regarded as the peri-infarct area where CBF-cerebral glucose metabolic rate (CMRglc) uncoupling was observed 24 h after embolization. In this paper, we examined the topography and temporal profile of COX-2 expression within 24 h of ischemia in a primate model of thromboembolic stroke using high-resolution PET.

Nine adult male cynomolgus monkeys weighing 3.4–4.3 kg were used in this study. All procedures were approved by our Institutional Animal Care and Use Committee, and were performed in accordance with the standards published by

* Corresponding author. Tel.: +81-6-6833-5012; fax: +81-6-6872-8091.
E-mail address: cyokota@ri.ncvc.go.jp (C. Yokota).

0304-3940/03/$ - see front matter © 2003 Elsevier Science Ireland Ltd. All rights reserved.
doi:10.1016/S0304-3940(03)00152-6

the National Research Council (Guide for the Care and Use of Laboratory Animals). Permanent focal ischemia was produced by carotid arterial embolization as previously described [7]. The monkeys were randomized into three groups of three animals. Animals in group I (normal control) did not undergo arterial embolization. Animals in group II underwent permanent focal ischemia for 2 h, while those in group III underwent permanent focal ischemia for 24 h. COX-2 expression in postmortem brains obtained from each group was investigated by biochemical means. In group III, CBF and the CMRglc were evaluated using high-resolution PET. Each animal was anesthetized by sevoflurane inhalation [0.5–2.0% sevoflurane delivered in a N_2O/O_2 (70%/30%) gas mixture] and was artificially ventilated. Body temperature was monitored and maintained at around 37 °C with the aid of heating pads.

The PET studies were performed with a multi-slice PET scanner (ECAT EXACT HR/47, Siemens/CTI, Knoxville, TN) [12], which provided 47 tomographic images at 3.1 mm intervals per frame. The spatial resolution at the center of the field of view was 3.7 mm in-plane at full width at half maximum and 4.1 mm axially. CBF and CMRglc were determined using ^{15}O-labeled water (^{15}O-H_2O) and 2-[^{18}F]fluoro-2-deoxy-D-glucose, respectively, and data analysis was performed according to the methods described previously [8]. To control for potential problems that arise as a result of the repeated withdrawal of blood during prolonged periods of experimentation, as a result of the effects associated with variations in levels of anesthesia, and as a result of partial volume effects [2], we expressed our results in terms of asymmetry index (AI), which was defined as the ratio of the value of regional CBF in the ROIs in the ischemic hemisphere to that in the contralateral homologous ROIs.

All animals were sacrificed by exsanguination following perfusion with ice-cold saline under pentobarbital anesthesia. Each brain was quickly removed and stereotaxically divided on ice into three slices corresponding to the coronal PET images as the same manner as the previous study [8]. Samples were extracted from the temporal cortices, parietal cortices, and basal ganglia, the size of which were 1 × 1 cm (width × height; Fig. 1A). Each sample was subdivided into two 4 mm (depth) pieces, which were dissected out from each slice from both ischemic and non-ischemic temporal lobe sections – one piece (>60 mg) was used for biochemical examination while the other was used for histopathological analysis.

RNA blot analysis was performed as previously described [6]. Total RNAs were prepared from samples derived from the second slice from both sides of animals in each group. In one animal in group II, total RNAs were also prepared from samples in each of the three slices from the ischemic side. The amount of COX-2 mRNA in each region was expressed as the ratio of the COX-2 mRNA signal to the glyceraldehyde-3-phosphate dehydrogenase (GAPDH) mRNA signal in that region (expression ratio).

Paraffin-embedded brain sections (3 μm thick), which were taken from the second slice from the ischemic hemispheres in groups II and III, and second slice from the left hemispheres in group I, were deparaffinized and incubated with a polyclonal COX-2 antibody (Cayman Chemical, Ann Arbor, MI; dilution 1:100) for 2 h at room temperature. After sections were washed with phosphate-buffered saline, biotinylated goat serum against rabbit IgG (Vector Laboratories, Burlingame, CA) was applied and the sections were incubated for at least 30 min at 25 °C. Immunoreactive signals were visualized using diaminobenzidine as the chromogen in a peroxidase reaction (Vectastain Elite Kit, Vector Laboratories).

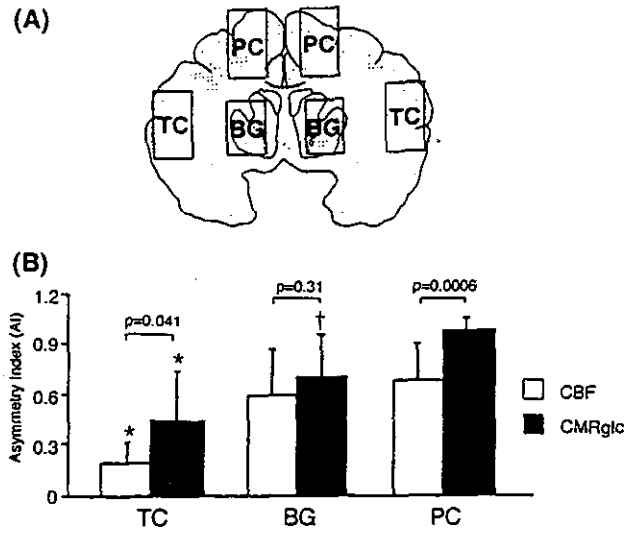

Fig. 1. (A) Manner of sample preparation. The brain was stereotaxically divided on ice into three slices corresponding to coronal PET images: the first rostral slice was a coronal cut at 23 mm from the frontal pole and another two slices were cut at 9 mm intervals parallel to the first slice. From each slice, both the ischemic and the non-ischemic temporal cortices (TC), parietal cortices (PC), and the basal ganglia (BG) were dissected out. (B)AIs for CBF and CMRglc following 24 h of focal ischemia. AIs for both CBF and CMRglc in the TC were reduced significantly (*) compared to those in the BG and PC. In the basal ganglia, AIs for CMRglc were also reduced significantly (†) compared to those in the parietal cortex. Results from a two-way analysis of variance that was used to assess the significance of differences in the AIs between CBF and CMRglc were: $P = 0.041$, $P = 0.31$, and $P = 0.0006$ for the temporal cortex, the basal ganglia, and the parietal cortex, respectively.

During the PET studies, physiological parameters including mean blood pressure, blood gases, and body temperature were maintained within the normal range. There were no significant differences in AIs for both CBF and CMRglc among the three slices from each site i.e. temporal cortex, parietal cortex, and basal ganglia. Significant reductions in AIs for CBF as well as CMRglc were demonstrated in the temporal cortex compared to those in the basal ganglia and parietal cortex (Fig. 1B). In the basal ganglia, AIs for CMRglc were also significantly reduced compared to those in the parietal cortex. On the other hand, the mean AI for CMRglc was preserved in the parietal cortex, whereas the mean AI for CBF was found to be reduced.

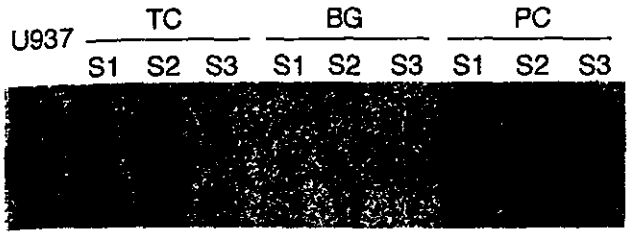

TC: temporal cortex, BG: basal ganglia, PC: parietal cortex
S1: slice 1, S2: slice 2, S3: slice 3

Fig. 2. RNA blot analysis of COX-2 expression following 2 h of ischemia in group II. COX-2 mRNA expression was detected in each region from the ischemic side. COX-2 mRNA expression in the ischemic parietal cortex was prominent, while expression in the ischemic basal ganglia was faint.

COX-2 mRNA expression following 2 h of ischemia (group II) was detected in each region from the ipsilateral hemisphere (Fig. 2). Expression of COX-2 mRNA in the first (slice1) and second (slice2) slices from the ischemic temporal cortex and in all slices (slice1, slice2, slice3) from the ischemic parietal cortex, was detected specifically as a single band (4.5 kb), the size of which was similar to that of human COX-2 mRNA extracted from lipopolysaccharide-treated U937 cells [5]; expression in the ischemic basal ganglia was faint. Expression of COX-2 mRNA in normal controls (group I) was as low as that on the side contralateral to the arterial embolization (Table 1). Expression ratios of COX-2 mRNA in group II were high in the ipsilateral cortices compared to those in group I. In group III, COX-2 mRNAs were undetectable in the ischemic temporal cortices and there were marked reductions in GAPDH mRNA expression, while expression ratios of COX-2 mRNA in the parietal cortex ipsilateral to the arterial embolization were prominently upregulated to the same levels as those seen in group II. Localized COX-2 immunoreactive neurons were detected predominantly in the ischemic parietal cortex in group III, while a few immunoreactive neurons were also observed in the ischemic temporal cortex and basal ganglia in group II. These immunoreactive neurons showed intense immunoreactivity in their cell bodies and apical dendrites (Fig. 3).

Fig. 3. Induction of COX-2 immunoreactive neurons in the parietal cortex in primate focal ischemia. Scale bar: 100 μm. Neuronal cell bodies and (apical) dendrites showed COX-2 immunoreactivity.

Table 1
Comparison of expression ratios of COX-2 mRNA between the three groups[a]

	Group I	Group II		Group III	
		ipsi	contra	ipsi	contra
Temporal cortex	0.83	11.83	0.69	–	0.60
	0.69	3.41	1.38	–	0.93
	0.45	6.97	1.57	–	0.38
Mean ± SD	0.66 ± 0.19	7.40* ± 4.23	1.21 ± 0.46	–	0.64 ± 0.28
Basal ganglia	0.33	1.03	0.66	–	0.55
	0.84	0.67	0.69	3.88	0.33
	0.13	3.91	0.93	2.07	0.28
Mean ± SD	0.43 ± 0.37	1.87 ± 1.78	0.76 ± 0.15	2.98 ± 1.28	0.39 ± 0.14
Parietal cortex	0.62	5.77	1.02	5.87	1.01
	0.65	4.44	1.49	2.62	0.87
	0.39	4.00	1.11	4.85	0.86
Mean ± SD	0.55 ± 0.14	4.74** ± 0.92	1.21 ± 0.25	4.45** ± 1.67	0.91 ± 0.08

[a] Group I indicates normal control. Animals in group II underwent permanent focal ischemia for 2 h, and those in group III underwent permanent focal ischemia for 24 h. Samples from three animals were used except in group III – ipsilateral (ipsi), basal ganglia – which were derived from only two animals because of a marked reduction in expression of both COX-2 and GAPDH mRNA. COX-2 transcripts were undetectable in all three samples from ipsilateral, temporal cortices in group III (–). A one-way analysis of variance was used to assess the significance of differences in the expression ratios between the three groups. *significantly higher than the temporal cortex in group I and temporal cortices contralateral (contra) to the arterial embolization in groups II and III ($P < 0.05$). **significantly higher than the parietal cortex in group I and parietal cortices contralateral (contra) to the arterial embolization in groups II and III ($P < 0.05$).

In the present study, we observed COX-2 expression during focal brain ischemia in a primate thromboembolic stroke model in which regional CBF and CMRglc were evaluated using high-resolution PET scanning. In this model, a reduction was observed in CBF in the ischemic temporal cortex and basal ganglia to <40% of the CBF in the contralateral hemisphere 1 h following embolization, while CBF in the ischemic parietal cortex was found to be >40% of contralateral values; these results support previous findings [7,8]. The flow threshold for infarct development was 12–15 ml $100g^{-1}$ min^{-1} (40% of contralateral values) in this model [8].

Our finding of an increase in COX-2 mRNA expression following focal brain ischemia that was demonstrable in the hemisphere ipsilateral to the arterial embolization, was consistent with previous findings in rodent models [1,9,10]. In the ischemic core in which a significant decrease in CBF were accompanied by reduced CMRglc, the upregulation in COX-2 mRNA expression that was seen following 2 h of ischemia decreased by 24 h of ischemia. The disappearance of COX-2 following 24 h of ischemia paralleled the reduction in expression of mRNA for the house-keeping gene, GAPDH, which indicated that ischemic injury was already apparent at this time in the basal ganglia as well as in the temporal cortex, a finding that is consistent with our previous report [8]. On the other hand, in the peri-infarct area, induced expression of COX-2 mRNA was still present following 24 h of ischemia in the parietal cortex, as was a mild CBF reduction, though CMRglc was maintained. Delayed induction of COX-2 in the infarcted human brain was suggested to promote reconstitutive processes in the form of tissue scarring and remodeling of the surviving neural networks [11]. Although interpretation of the results in this study should be careful because of the limited number of primates, we propose that the regulation of COX-2 expression is different in the ischemic core than in the peri-infarct area, and that therefore the role of COX-2 in focal ischemic tissues is determined by the depth and duration of CBF reduction.

Acknowledgements

We are grateful to Dr Takeo Abumiya for his suggestions concerning the preparation of this manuscript, and thank Mr. Norimasa Ejima and Miss Yumi Miyamoto for their technical assistance. This work was supported in part by Special Coordination Funds for Promoting Science and Technology (Strategic Promotion System for Brain Science) from the Ministry of Education, Culture, Sports, Science and Technology of Japan, by a Grant-in-Aid for Scientific Research from the Japan Society for the Promotion of Science, by a Grant from Japan Heart Foundation Research, by a Grant from the Takeda Medical Research Foundation in Japan, and by Research Grants for Cardiovascular Diseases (11C-3, 12A-2) from the Ministry of Health, Labor and Welfare of Japan.

References

[1] Y. Collaco-Moraes, B. Aspey, M. Harrison, J.D. Belleroche, Cyclo-oxygenase-2 messenger RNA induction in focal cerebral ischemia, J. Cereb. Blood Flow Metab. 16 (1996) 1366–1372.
[2] W.-D. Heiss, R. Graf, K. Wienhard, L.R. Saito, T. Fujita, G. Rosner, R. Wagner, Dynamic penumbra demonstrated by sequential multitracer PET after middle cerebral artery occlusion in cats, J. Cereb. Blood Flow Metab. 14 (1994) 892–902.
[3] C. Iadecola, C. Forster, S. Nogawa, H.B. Clark, M.E. Ross, Cyclooxygenase-2 immunoreactivity in the human brain following cerebral ischemia, Acta. Neuropathol. 98 (1999) 9–14.
[4] C. Iadecola, K. Niwa, S. Nogawa, X. Zhao, M. Nagayama, E. Araki, S. Morham, M.E. Ross, Reduced susceptibility to ischemic brain injury and *N*-methyl-D-aspartate-mediated neurotoxicity in cyclooxygenase-2-deficient mice, Proc. Natl. Acad. Sci. USA 98 (2001) 1294–1299.
[5] H. Inoue, T. Tanabe, K. Umesono, Feedback control of cyclooxygenase-2 expression through PPARgammma, J. Biol. Chem. 275 (2000) 28028–28032.
[6] H. Inoue, C. Yokoyama, S. Hara, Y. Tone, T. Tanabe, Transcriptional regulation of human prostaglandin-endoperoxide synthase-2 gene by lipopolysaccharide and phorbol ester in vascular endothelial cells, J. Biol. Chem. 270 (1995) 24965–24971.
[7] G. Kito, A. Nishimura, T. Susumu, R. Nagata, Y. Kuge, C. Yokota, K. Minematstu, Experimental thromboembolic stroke in cynomolgus monkey, J. Neurosci. Methods 105 (2001) 45–53.
[8] Y. Kuge, C. Yokota, M. Tagaya, Y. Hasegawa, A. Nishimura, G. Kito, N. Tamaki, N. Hashimoto, T. Yamaguchi, K. Minematsu, Serial changes in cerebral blood flow and flow-metabolism uncoupling in primates with acute thromboembolic stroke, J. Cereb. Blood Flow Metab. 21 (2001) 202–210.
[9] S. Miettinen, F.R. Fusco, J. Yrjanheikki, R. Keinanen, T. Hirvonen, R. Roivainen, M. Narhi, T. Hokfelt, J. Koistinaho, Spreading depression and focal brain ischemia induce cyclooxygenase-2 in cortical neurons through *N*-methyl-D-aspartic acid-receptors and phospholipase A2, Proc. Natl. Acad. Sci. USA 94 (1997) 6500–6505.
[10] S. Nogawa, F. Zhang, M.E. Ross, C. Iadecola, Cyclo-oxygenase-2 gene expression in neurons contributes to ischemic brain damage, J. Neurosci. 17 (1997) 2746–2755.
[11] T. Sairanen, A. Ristimaki, M.-L. Karjalainen-Lindsberg, A. Paetau, M. Kaste, P.J. Lindsberg, Cyclooxygenase-2 induced globally in infarcted human brain, Ann. Neurol. 43 (1998) 738–747.
[12] K. Wienhard, M. Dahlbom, L. Eriksson, C. Michel, T. Bruckbauer, U. Pietrzyk, W.D. Heiss, The ECAT EXACT HR: performance of a new high resolution positron scanner, J. Comput. Assist. Tomogr. 18 (1994) 110–118.
[13] K. Yamagata, K.I. Andreasson, W.E. Kaufmann, C.A. Barnes, P.F. Worley, Expression of a mitogen-inducible cyclooxygenase in brain neurons: regulation by synaptic activity and glucocorticoids, Neuron 11 (1993) 371–386.